Chem Soc Rev

Carbon-Fluorine Bond Cleavage Mediated by Metalloenzymes

Journal:	*Chemical Society Reviews*
Manuscript ID	CS-SYN-10-2019-000740.R3
Article Type:	Review Article
Date Submitted by the Author:	12-May-2020
Complete List of Authors:	Wang, Yifan; University of Texas at San Antonio, Chemistry Liu, Aimin; University of Texas at San Antonio, Chemistry; Prof

SCHOLARONE™
Manuscripts

Carbon-Fluorine Bond Cleavage Mediated by Metalloenzymes

Yifan Wang and Aimin Liu*

Department of Chemistry, University of Texas at San Antonio, 1 UTSA Circle, San Antonio, TX 78249, U.S.A.

*To whom correspondence should be addressed:

Aimin Liu

Department of Chemistry

The University of Texas at San Antonio

One UTSA Circle

San Antonio, TX 78249, USA

Tel: +1-210-458-7062

E-mail: Feradical@utsa.edu

Abstract

Fluorochemicals are a widely distributed class of compounds and have been utilized across a range of industries for decades. Given the environmental toxicity and adverse health threat of some fluorochemicals, the development of new methods for decomposition is of great interest to public health. However, the carbon-fluorine (C–F) bond is among the most chemically robust bonds; and consequently, the degradation of fluorinated hydrocarbons is exceptionally difficult. Here, metalloenzymes that catalyze the cleavage of this chemically challenging bond are reviewed. These enzymes include histidine-ligated heme-dependent dehaloperoxidase and tyrosine hydroxylase, thiolate-ligated heme-dependent cytochrome P450, and four non-heme oxygenases including tetrahydrobiopterin-dependent aromatic amino acid hydroxylase, 2-oxoglutarate-dependent hydroxylase, Rieske dioxygenase, and thiol dioxygenase. Whilst much of the literature regarding the aforementioned enzymes highlights their ability to catalyze C–H bond activation and functionalization, in many cases, C–F bond cleavage has been shown to occur on the fluorinated substrates. A copper-dependent laccase-mediator system representing an unnatural radical defluorination approach is also covered. Detailed discussions on structure-function relationships and catalytic mechanisms provide insight into biocatalytic defluorination, which may inspire drug design considerations and environmental remediation of halogenated contaminants.

Keywords: C–F bond cleavage; C–H bond activation and functionalization; dehalogenation; fluorine chemistry; free radical; mechanistic enzymology; and redox chemistry.

1. Introduction

Fluorine-containing hydrocarbons, also known as organofluorine compounds, are widely spread in our daily life. Fluorine substitution is known for its small steric effect, highly electron-withdrawing property, lipophilicity and thermal stability.[1-3] The unique chemical properties of fluorine have spawned applications of organofluorines in diverse fields, including material, pharmaceutical, catalysis, energy, and agriculture.[1-4] Human civilization has greatly profited from the development and manufacture of fluorinated compounds. The fluorochemical market was valued at 24.6 billion USD with a global production volume of 4.2 million tonnes during 2018.[5] It was also reported that about 30% of the approved drugs are fluorine-containing compounds.[6] Nevertheless, a significant characteristic of these fluorocarbon compounds is the strength of the carbon-fluorine (C–F) bond. For instance, the bond dissociation energy of C–F bond in fluorobenzene is 526 J/mol.[7] To break such a chemically robust bond in a homolytic process is difficult under mild conditions. As a result, the prevalence and accumulation of fluorinated compounds, especially perfluorinated compounds, is becoming a severe, worldwide environmental threat.[8-13] Of the most concerned fluorochemicals, per- and polyfluoroalkyl substances (PFAS) are manufactured and used widely, but some are now globally banned due to their adverse health effects.[14] These chemically inert carcinogens, once released, are challenging to decompose in the natural environment and thus, result in significant contamination in soil and ground water.[15]

Consequently, the degradation of fluorochemicals has attracted considerable attention and inspired research work on C–F bond activation and cleavage. In recent years, various model complexes have been synthesized and shown to perform C–F bond cleavage by employing metals such as Fe, Al, Cu, Mn, and even some rare earth metals.[16-24] In most cases, it has been proposed that high-valent metal-oxo species play a critical role in the catalytic mechanism of these metal

complexes.[18, 22, 25] Currently, the primary methods for defluorination are the use of synthetic

models and artificial catalysts, while the exploration of biocatalysts is still in its infancy. Although

C–F bond cleavage requires a considerable input of energy, microorganisms that have adapted to

polluted environments have been found to facilitate the biodegradation or biotransformation of

fluorinated compounds.[26-28] Studies on these microbial types of machinery have revealed several

enzymes capable of C–F bond cleavage.[27, 29-31] In addition to the proteins identified in the

catabolism of the microorganisms, there are other enzymes found to exhibit substrate promiscuity

when confronted with noncanonical, fluorinated substrates.[32-37] These findings provide a

promising platform to engineer biocatalysts that detoxify fluorochemicals. In general, these

defluorinase proteins can be classified into two groups, metal-independent, and metal-dependent

enzymes. Examples for metal-independent systems are fluoroacetate dehalogenases,[38-40] ATP-

dependent reductases, [41, 42] certain hydroxylases and isomerases [43-46] and flavin-dependent

monooxygenases.[47-49] Metal-containing proteins with or intimately associated with C–F bond

cleavage activities have been elucidated and are increasingly appreciated. Metalloenzymes are

proficient catalysts due to their oxygen activation activity, substrate selectivity, specificity, and

structural stability. The formation of high-valent metal intermediates during catalysis empowers

these proteins to mediate a broad spectrum of chemistries, including defluorination. In this review,

metalloprotein-mediated defluorination, mostly on fluoroaromatics, is summarized. These

metalloenzymes activate C–H bonds and are relevant to essential metabolism events, while C–F

bond cleavage can take place on fluorinated substrates *via* distinguishing routes. Herein, the C–F

bond cleavage reactions will be discussed in detail in terms of the molecular mechanism. It is

expected that the study of enzymatic structure-function relationship coupled with knowledge of

the catalytic mechanism will shed light on defluorination chemistry and pave the way for future applications.

2. C–F Bond Activation by Histidine-Ligated Heme Enzymes

2.1. Histidine-Ligated Heme-Dependent Dehaloperoxidase

Metalloenzyme-mediated defluorination is a rare catalytic transformation across the biosynthesis of natural metabolites. However, the multifunctional globin-like protein dehaloperoxidase (DHP) is a well-characterized example of an enzyme capable of promoting such chemistry. DHP was originally discovered in *Amphitrite ornata*, a marine polychaete worm of the family Terebellidae.[50] Other than binding and transporting molecular oxygen as hemoglobin, DHP has long been known to have multiple catalytic properties including activity typical of an oxygenase, an oxidase, a peroxygenase and even a peroxidase for dehalogenation.[51-53] Herein, we will focus on discussing the peroxidase activity of the enzyme.

DHP oxidizes trihalophenols (TXP) to their corresponding quinones by utilizing hydrogen peroxide as a co-substrate, resulting in the elimination of the *para*-substituted halogen (F, Cl, Br or I) on TXP in the form of a halide anion, as shown in **Figure 1A**. In the resting state, DHP possesses a histidine-ligated *b*-type ferric heme (**Figure 1B**), and an overall fold typical of the globin family.[54] The enzyme is predominantly dimeric in solution, and it crystallizes as a dimer in an asymmetric unit.[30] The crystal structures of DHP in complex with substrate analogues or inhibitors depict diverse binding modes in the active site, indicative of spacious substrate cavity.[55-58] The crystal structures of the enzyme-substrate (ES) complexes were determined by soaking with a native substrate, tribromophenol (TBP). However, the occupancy of TBP is extremely low in the determined ES complex structures (occupancy ~10%, PDB entries: 4FH6 and 4FH7).[56] Although

the structures of the ES complex are contentious due to the low occupancy, TBP is shown to bind in the active site with its hydroxyl group pointing towards the heme center, while the *para*-substituent to be eliminated points away (**Figure 1B**). This structural information excludes the possibility of a direct activation on the *para* position by a heme-based oxidant during the catalytic reaction.

The dehalogenation mechanism of DHP is presumed to involve two one-electron oxidation processes mediated by the high-valent heme iron oxidants, *i.e.*, the Compound I (Cpd I)- and II (Cpd II)-like species, respectively.[59-62] Cpd I and Cpd II represent two reactive ferryl-oxo intermediates in the catalytic cycle of thiolate-ligated cytochrome P450 with the former containing a porphyrin-based cation radical but absent in the latter. These high-valent species, or their equivalents with a histidine-ligated heme, are commonly proposed oxidants in the catalytic pathways of the heme-containing enzymes.[63, 64] **Figure 2** depicts the proposed defluorination mechanism of DHP. Even though the binding order of TXP and H_2O_2 are inconclusive,[55, 65] it is believed that the conformational flexibility of a distal histidine, His55, plays a critical role in adopting an activated DHP.[66, 67] In the activated form, His55 is in close contact with the heme center, as shown in **Figure 1B**. The protein then promotes heterolytic cleavage of the O–O bond by providing a proton to the ferric hydroperoxo, resulting in a histidine-ligated Cpd I-like species.[65, 68] Such a species is chemically equivalent to the so-called Compound ES (Cpd ES), which is a Cpd I isoform with a ferryl heme and a nearby protein-based aromatic radical.[69, 70] Subsequently, Cpd I or Cpd ES proceeds with the first one-electron oxidation of the substrate, yielding a dissociable organic radical on the substrate and a Cpd II-like species.[71, 72] The Cpd II-like species then performs the second one-electron oxidation on a resonance structure of the substrate radical to generate a phenoxy cation. Formation of the stable 2,6-difluoro-quinone product is through the

elimination of fluoride, which occurs after nucleophilic attack by a water molecule at the *para*-substituted carbon atom bearing the most cationic character.[57, 71] [18]O isotope labeling studies confirm that the oxygen atom incorporated to the final product is derived from water rather than peroxide, consistent with the binding orientation of substrate revealed by crystal structures.[57]

Although DHP functions as a natural dehalogenase that oxidizes phenols with various halogen substituents, affinity studies, and catalytic efficiency have shown that DHP favors brominated substrates under physiological conditions.[50, 73] Fluorinated phenols, on the other hand, have weak binding affinities and limited turnovers.[50, 58, 73] However, the construction of an artificial DHP could be a promising method to develop competent biocatalysts that effectively cleave aromatic C–F bonds. Indeed, artificially created DHP activity has been achieved by mutating active site residues in structurally related myoglobin.[74] Although the defluorination activity of the native protein is yet to be reported, the engineered enzyme demonstrates a 1,000-fold increase in efficiency on the substrate trichlorophenol. Consequently, engineered DHP is a prime candidate for defluorination activity, which provides promise that residue level modification is an effective strategy to achieve engineered enzymatic C–F bond cleavage of harmful fluorinated compounds.

2.2.   Histidine-Ligated Heme-Dependent Tyrosine Hydroxylase

A new class of biocatalysts hydroxylating L-tyrosine to L-dihydroxyphenylalanine (DOPA) has been found in the biosynthetic pathways of antitumor and/or antibacterial antibiotics.[75] While their protein structures remain to be determined, these tyrosine hydroxylases are heme-dependent proteins, and hence hereafter referred to as heme TyrHs. The protein sequence analysis suggests this type of enzymes containing a *b*-type histidine-ligated heme.[76, 77] The first of this class of enzyme, LmbB2, was identified from the biosynthetic gene cluster of lincomycin.[78] In addition to

LmbB2, other characterized heme TyrHs include HrmE of hormaomycin,[79] Orf13 of anthramycin,[76] SibU of sibiromycin,[80] TomI of tomaymycin,[81] and Por14 of poranthramycin.[82] The amino acid sequence alignment of these TyrHs shows no similarity with any known conserved domains or conserved motifs,[76] and thus, this group of proteins likely containing a novel structural fold and determining the structural features of this enzyme family is imperative for mechanistic understandings. The heme-dependent TyrH is responsible for the first step in the construction of the pyrroline moiety in the natural product biosynthetic pathways by converting L-tyrosine to DOPA through a hydrogen peroxide mediated oxidation. Unlike thiol-ligated cytochromes P450, non-heme TyrH, and other aromatic hydroxylases,[83-87] the catalytic heme in TyrHs are distinguished by an axial histidine ligand. Thus, their mechanism of C–H bond activation and oxygen atom transfer cannot be simply extrapolated.[32]

LmbB2 has been shown to be capable of hydroxylating a range of L-tyrosine analogues with ring-deactivating *meta*-substituents such as 3-fluoro-tyrosine.[32] Moreover, in addition to the expected C–H bond cleavage product, an additional product derived from C–F bond cleavge has also observed (**Figure 3A**). A C–F bond cleavage requires two additional electrons for fluoride versus proton elimination, hence the mechanism of C–F bond hydroxylation is likely to differ from the native C–H bond hydroxylation. Consumption of additional peroxide and formation of oxygen were found in the process of C–F bond cleavage, which suggests that oxidation of peroxide to oxygen presumably provides as the source of the two necessary electrons. Moreover, ^{18}O isotope labeling experiments support that H_2O_2 is the oxygen source for hydroxylation in both C–H and C–F bond cleavage reactions. Detection of the double-scrambled product (with ^{18}O atoms on both hydroxyl groups of DOPA) indicates a potential ketone or radical intermediate with broken

aromaticity during catalysis. Collectively, a mechanism of C–F bond cleavage promoted by the heme-dependent TyrH was proposed (**Figure 4**).

Substrate binding to the active site allows for hydrogen peroxide activation by the ferric heme to generate a ferric-bound hydroperoxide. It has been speculated that 3-fluoro-tyrosine can bind in the active site with two distinct conformations, with the fluorine pointing towards or away from the heme center.[32] Fluorine pointing away from the heme would result in the native hydroxylated product, while fluorine orienting towards the heme results in the defluorinated product. In the latter case, due to the strong electron-withdrawing property of the fluorine substituent, the covalently bound carbon (C3) is partially electropositive. Thus, ferric heme-bound hydroperoxide can perform a nucleophilic attack at C3, resulting in a Cpd I-like species. In contrast to the alkyl systems, fluoride is an excellent leaving group in a nucleophilic aromatic substitution reaction.[88] It is eliminated from the ring to re-aromatize, yielding DOPA as the final product. The resulting Cpd I-like species will react with an additional equivalent of H_2O_2 to release oxygen and return to the resting state via catalase-like activity. Besides 3-fluoro-tyrosine, 3-chloro- and 3-iodo-tyrosine have also been identified with dual reactivities. 3-Chloro-tyrosine has the best overall conversion (normal hydroxylation plus dehalogenation). At the same time, 3-fluoro-tyrosine exhibits the highest dehalogenation efficiency, despite the C–F bond being the most durable among all carbon-halogen (C–X) bonds. The different distribution of hydroxylated products from two distinct reaction pathways is a cumulative outcome of the steric and inductive effect of these halogen substituents.

Cleaving an aromatic C–F bond is not a common feature among the histidine-ligated heme proteins because they typically function as globins or peroxidases to bind oxygen or transfer electrons. But a closer comparison between DHP and heme TyrH suggests these two enzymes

catalyze very different dehalogenation reactions (**Table 1**), even though they utilize the same biocatalytic cofactor and oxidant (H_2O_2). In the case of DHP, the *para*-substituted halogen is eliminated from the phenyl ring via a two-electron oxidation process, resulting in dissociation of the halide and formation of a quinone. The oxygen atom incorporated into the quinone is from a water molecule. In contrast, besides C–H bond cleavage, the heme TyrH promotes the elimination of the *meta*-substituted halogen via non-oxidative hydroxylation to generate catechol and halide. Additionally, the order of dehalogenation reactivity of heme TyrH inversely reflects the size of the halogen atoms, whereas the opposite is true in DHP. Such contrary results indicate that the governing factor of the catalysis is distinct between these two enzymes, which can be explained by their distinct key oxidants, *i.e.,* the Cpd I-like species for DHP and ferric-bound hydroperoxo for heme TyrH, respectively.

3. C–F Bond Cleavage by Thiolate-Ligated Cytochrome P450

The cytochrome P450 enzymes (CYPs) constitute a remarkable superfamily of monooxygenases that are ubiquitously present in all kingdoms of life and even viruses.[89] Notably, they are found in all mammalian tissues and are most abundant in the liver and small intestine, which participate in the metabolism of endogenous compounds, environmental pollutants, and carcinogens. For instance, there are at least 57 CYP genes found in humans thus far, and five of the corresponding CYPs, CYP 1A2, 2C9, 2C19, 2D6, and 3A4, are responsible for 90% of the oxidation of commercial drugs.[90, 91]

With such prevalence and importance, the structures and functions of CYPs have been relatively well characterized. Compared with histidine-ligated heme enzymes, thiolate-ligated CYPs have a wider substrate specificity and promote a much broader spectrum of chemical

reactions, *e.g.,* hydroxylation, heteroatom oxygenation, oxidation, epoxidation, dealkylation, dehalogenation, desaturation, desulfurization, C-C bond forming, C-C bond clavage, and *O*-demethylation, *etc*.[91-93] Although the mechanism varies in specific reactions, they share the same procedure to generate the common reactive intermediates, namely Cpd I and II.[63, 64] As aforementioned, both Cpd I and II contain a ferryl-oxo intermediate, but differ by one electron in the oxidation state of the porphyrin. These ferryl species are almost exclusively responsible for the majority of the chemistry mediated by P450 enzymes. The active site of CYPs contains a proximal cysteine-ligated heme iron, usually deeply buried inside the protein with an access channel connecting it to the protein surface.[91, 94] Substrate binding induces a conformational change in the active site, triggering electron transfer from NADPH by NADPH-dependent cytochrome P450 reductase or cytochrome b_5. Subsequently, an oxygen molecule binds the ferrous heme and is activated to promote heterolytic cleavage of O–O bond, resulting in Cpd I (**Figure 5**). The following substrate activation then branches off to different reactions after the formation of Cpd I oxidant. Compared with other metalloenzymes, CYPs are more frequently reported to perform defluorination reactions, typically on drugs or other small molecules: CYP 1A2 and 3A4 catalyzed aromatic C–F bond hydroxylation on drugs such as Sunitinib and Famitinib to release reactive, potentially toxic metabolites;[95, 96] The CYP-mediated defluorination on imaging tracers have been reported from the *in vivo* studies;[97, 98] human liver CYPs defluorinate the inhaled anesthetics such as halothane and sevoflurane to generate toxic metabolic intermediates;[99-101] multiple bacterial or mammalian liver CYPs have shown significant oxidative defluorination activity on the *para* position of fluorinated phenol or aniline, and producing quinone or quinone imine and corresponding halide anion.[102-107]

The mechanism of P450-mediated oxidative aromatic defluorination is illustrated using *para*-fluorinated phenol as an example (**Figure 3B**). The most plausible defluorination proposal involves an electrophilic attack of the substrate to Cpd I, as shown in **Figure 5**.[63, 103, 105] Considering the electron-rich nature of the phenol, once Cpd I is formed in the active site, it readily performs an electrophilic attack on a nearby substrate producing a transient cationic intermediate, as is proposed in the non-heme TyrH catalytic mechanism discussed in the following section. Rearrangement of the cationic adduct promotes heterolytic Fe–O bond cleavage to generate benzoquinone and fluoride, allowing heme to resume its resting state after releasing quinone. In the presence of NADPH or other reducing equivalents, hydroquinone can be observed due to the reduction of benzoquinone.[63, 102] Similarly, CYPs have dehalogenation activity on *para*-substituted chloro- and bromo- phenols as well, while fluorinated substrate yielded the most product of C–X bond cleavage.[103, 108, 109] It is worth noting that fluoride is a better leaving group in nucleophilic aromatic substitution, but not necessarily in the case of electrophilic substitution (see section 7 for details). If the reaction indeed proceeds through Cpd I-directed electrophilic attack, the observed effect of halogen substituent should be explained by other factors, such as steric hindrance and substrate binding affinity.

Additionally, some types of CYP-mediated defluorination reactions are found in metabolism to generate fluoride and resulting toxic metabolites, which can be triggered by *O*-demethylation, *N*-dealkylation, dealkylation, *ortho*-elimination of alcohol/amine, *etc*.[110] It is not entirely surprising considering the exceptional chemistries performed by the superfamily of CYPs. Hence, drug defluorination promoted by CYPs and the toxicity of resulting metabolites are indeed worthy of attention during the process of drug design, selection, optimization, and especially toxicology studies in the drug development process.

4. C–F Bond Functionalization by Non-Heme Iron Hydroxylases

4.1. Tetrahydrobiopterin-Dependent Aromatic Amino Acid Hydroxylase

Similar to heme-dependent enzymes, non-heme iron enzymes perform a multitude of oxidation chemistries. Like heme TyrH, a non-heme iron-dependent tyrosine hydroxylase (non-heme TyrH) also catalyzes the conversion of L-tyrosine to DOPA and such a non-heme TyrH is biologically more significant than its heme counterpart. As a rate-limiting step in the biosynthesis of catecholamines, the reaction requires molecular oxygen, and tetrahydrobiopterin (BH_4) as co-substrates (**Figure 6B**).[87, 111] One oxygen atom from molecular oxygen is inserted into the co-substrate BH_4, generating 4a-hydroxytetrahydropterin (4a-OH-BH_4). The other oxygen atom is incorporated into the aromatic ring of tyrosine. The active enzyme is a tetramer, and each of the subunits contains a ferrous iron coordinated by two histidines and one glutamate as a cofactor, shown in **Figure 6A**.[112, 113] In the resting state, water molecules comprise the remaining ligands in a distorted octahedral complex. In some instances, the enzyme is activated by BH_4 and oxygen but without a bound L-tyrosine, the enzyme can self-hydroxylate its phenylalanine residue, Phe300, to 3-hydroxyl-phenylalanine (3-OH-Phe300).[113] This alternative activity is likely an enzyme self-protection mechanism, as first found in TfdA[114] and then other non-heme iron enzymes, to prolong the enzyme activity during the undesired and uncoupled oxidation.[115-118] The current understanding of the catalytic mechanism of non-heme TyrH is based on a variety of biochemical and spectroscopic studies.[119-122] The hydroxylation reaction can be divided into two half-reactions. The first half-reaction involves BH_4 hydroxylation to generate 4a-OH-BH_4 and a ferryl-oxo intermediate. The second half-reaction starts with the high-valent iron species oxidizing tyrosine

through an electrophilic addition, resulting in an Fe(II)-bound cationic intermediate.[123] The proton than eliminates to liberate the final DOPA product in a natural reaction.

When 3-fluoro-tyrosine is used as a substrate in place of L-tyrosine, the hydroxylation reaction takes place only on C3 due to the small size of fluorine and, consequently, produces a defluorinated product, DOPA (**Figure 6C**). Notably, unlike heme TyrH, the reaction yields only the defluorinated product without hydroxylation at the C5 position. This selectivity may indicate that the active site recognizes and interacts specifically with the C3-substituent so that the mono-substituted tyrosine analogue has a single binding mode to the active site that only allows defluorination. Other 3-halogenated tyrosine analogues have the same outcome with dehalogenation efficiency of F > Cl > Br.[33] However, the products derived from halogen atoms and the detailed dehalogenation mechanism remain unknown. The likelihood of the formation of a fluorine cation or a fluorine radical is extremely low in a biological system. If the fluorine substituent eliminates as fluoride, as seen in most cases, the source of the additional electrons required relative to the C–H bond cleavage requires further investigation. The reaction stoichiometry of BH_4 in the 3-fluoro-tyrosine reaction may reveal the mystery. It is also unclear if the Fe(IV)-oxo species involved in the native C–H bond hydroxylation is responsible for C–F hydroxylation.

Interestingly, 4-halogenated phenylalanine can react with non-heme TyrH as well. With the exception of 4-fluorophenylalanine, which produces only tyrosine, challenging non-heme TyrH with either 4-chloro- or 4-bromophenylalanine generates multiple products as an outcome of the NIH shift and dual hydroxylation sites (C3 and C4). In the case of non-heme TyrH, NIH shift represents a 1,2-migration of the halogen functional group at the site of substitution in aromatic hydroxylation reactions. In addition to tyrosine, reactions on 4-chloro- and 4-bromo-

phenylalanine also yield 3-halo-tyrosine and 3-hydroxy-4-halo-phenylalanine as products (**Figure 6D**). Non-heme TyrH can hydroxylate at both C3 and C4 positions of 4-halogenated phenylalanine, depending on the size of the substituent at C4. It is proposed that hydroxylation at C3 results in 3-hydroxy-4-halo-tyrosine through the reaction route proposed for hydroxylation of L-tyrosine. Hydroxylation at the C4 position yields an Fe(II)-bound cationic intermediate, which can undergo either an NIH shift of the halogen substituent forming 3-halo-tyrosine or a direct halide elimination forming tyrosine.[33, 124] Here, 4-fluoro-phenylalanine is used to illustrate the defluorination catalyzed by non-heme TyrH (**Figure 7**). After the first half-reaction forming 4a-OH-BH$_4$ and ferryl-oxo intermediate, electrophilic substitution occurs only at C4 to generate an Fe(II)-bound cationic intermediate. Without an NIH shift, fluoride is directly eliminated to create the re-aromatized product, tyrosine. For 3-chloro and 3-bromo-substituted phenylalanine analogues, the ratio of hydroxylation at C3 and C4 is nearly 1:1. In the case of C4 hydroxylation, more NIH shift product (3-halo-tyrosine) is observed as the halogen atom size increases (Br > Cl >> F). With halogen elimination, tyrosine is generated (F > Br, Cl). However, the fate of the halogen upon elimination is unresolved although halide is the possible leaving agent of the reaction. There should be an electron source to provide the two necessary electrons and eventually generate halide as the final product. Unfortunately, neither such as electron donor nor the final halogen-containing product has been identified. Further mechanistic investigation on this system is needed in order to gain a better mechanistic understanding.

The non-heme TyrH has two other siblings. The mononuclear, non-heme, iron-dependent aromatic amino acid hydroxylases, phenylalanine hydroxylase (PheH), and tryptophan hydroxylase (TrpH), are also well studied. The three enzymes are all pterin-dependent hydroxylases and they share a significant degree of homology of the catalytic domains.

Spectroscopic data indicate their catalytic pathways may proceed through a similar Fe(IV)-oxo intermediate.[125-127] The defluorination activity of PheH on 4-fluorophenylalanine to tyrosine has been reported in an early study.[128] The formation of fluoride was detected, and the oxidation of BH_4 was proposed to provide the required electrons, which is a feasible explanation for the questions raised in TyrH system. Given the defluorination capacities of non-heme TyrH and PheH, it is reasonable to extrapolate that C–F bond cleavage is accessible by TrpH. Future studies on the activities and product distribution of fluorinated tryptophan analogues are anticipated.

Overall, the defluorination capacity of the non-heme iron enzyme TyrH is quite interesting. This enzyme can cleave the C–F bond at different sites when facilitated by oxygen addition via electrophilic substitution. The cationic intermediate is highly destabilized due to the fluorine substitution, which promotes the re-aromatization to cleave C–F bond. However, the nature of the fluorine elimination and potential electron source to balance the reaction require more investigation.

4.2. Non-Heme Iron Hydroxylase with 2-Oxoglutarate as the Co-substrate

As discussed in non-heme TyrH that utilizes both BH_4 and tyrosine as organic substrates, several non-heme iron, oxygen-dependent enzymes split dioxygen into two substrates through stepwise incorporation. Such an oxygen-activation method is also employed by a well-studied enzyme superfamily, 2-oxoglutarate-dependent hydroxylases. These enzymes are also non-heme iron dioxygenases that insert two oxygen atoms into a 2-oxoglutarate (2OG, also known as α-ketoglutarate) molecule and a primary substrate. Its catalytic Fe(II) center is coordinated by a 2-His-1-carboxylate facial triad and three water molecules, and the carboxylate group normally serves as a monodentate ligand.[129, 130] The co-substrate 2OG ligates to the iron center in a bidentate

fashion to replace two of the water molecules, which is followed by the binding of the primary

substrate nearby to displace the remaining water.

Such a binding order triggers dioxygen ligation and activation, yielding ferric ion-bound

superoxide. The distal oxygen of superoxide attacks the keto carbon of 2OG to form a bicyclic

intermediate with a peroxide bridge. Heterolytic O–O bond cleavage gives rise to an Fe(IV)-oxo

species and promotes the oxidative decarboxylation of 2OG to release CO_2. The Fe(IV)-oxo

species has been observed by spectroscopic methods.[131-134] After the oxygen transfer to the iron-

bound 2OG, the succinate product remains chelate to iron in a monodentate manner. The high

redox power of Fe(IV)-oxo species allows a hydrogen atom abstraction from the adjacent primary

substrate to generate ferric hydroxo and a substrate radical.[135] The second oxygen is delivered by

hydroxyl radical rebound to the substrate radical, forming the hydroxylated product. Dissociation

of the hydroxylated product and succinate from the active site completes the entire catalytic cycle.

It is noteworthy that the process of hydrogen atom abstraction and oxygen rebound in 2OG-

dependent hydroxylases bears a resemblance to the CYP-mediated hydroxylation. Such a typical

catalytic mechanism mediated by 2OG-dependent hydroxylases is well understood.[136, 137]

If the site of hydroxylation has a fluorine substituent on the carbon, the hydroxylation could

lead to defluorination after oxidation of the substrate as shown in prolyl hydroxylase.[138-140] Prolyl

hydroxylase is also a 2OG-dependent hydroxylase, which catalyzes a 3-, or 4-hydroxylation on

proline residues in diverse proteins.[137] Herein, our discussion will focus on prolyl-4-hydroxylase

(P4H). As one of the important oxygen-sensing mechanisms,[141-143] the oxygen-dependent proline

hydroxylation on hypoxia-inducible factor is an irreversible and stereoselective process, which

produces (2*S*,4*R*)-4-hydroxyproline (Hyp) in the target protein (**Figure 8A**). The substrate

multiplicity of P4H reveals the wide distribution and various biological functions of the Hyp-

presented proteins. Thus far, different P4Hs have been found to alter protein conformation, tune enzymatic stability and activity, prepare for further modifications, as well as promote protein–protein interactions.[144, 145] Two biologically essential examples are a hypoxia-inducible factor (HIF)- and collagen-related P4Hs, and both are considered as important therapeutic targets.[146-148] The cellular adaptation to hypoxia involves the expression of multiple genes regulated by HIFs. Under hypoxic conditions, low oxygen availability limits the hydroxylation activity of P4H on prolyl residues of HIFs and thus prevents signaling for proteasomal degradation of HIFs.[148-150] Like all 2OG-dependent hydroxylases, P4H binds 2OG in a bidentate fashion, and the target proline residue locates nearby (**Figure 8B**). In this particular structure, P4H is substituted with manganese and is in complex with a fragment of HIF with a Pro564 to be readily oxidized.[150]

Collagen is a dominant protein of the extracellular matrix, which is composed of a three-stranded helix of high tensile strength.[151] As the significant connective tissue of the human body, its stability is significantly increased by the formation of Hyp due to the establishment of water bridges and/or stereoelectronic effects.[34, 145, 146, 151] Studies have shown that incorporation of (2*S*,4*S*)-4-fluoroproline (Flp) to collagen in place with Hyp results in increased thermostability.[34, 152] However, the incorporation of Flp is not guaranteed in the presence of P4H due to its defluorination activity (**Figure 8C**).[138-140] After the formation of hydroxylated Flp though the typical 2OG-dependent hydroxylation mechanism, the fluorine can be spontaneously eliminated from the hydroxylated product and generate (2*S*)-4-keto-proline (Kep) as the final product (**Figure 9**). The elimination of fluoride rather than hydroxide is because fluoride is a much better leaving group. The steady-state kinetic parameters of an Flp-containing peptide are comparable to the natural substrate, which indicates the rearrangement of the hydroxylated product to defluorination

is not a rate-limiting step. The dehalogenation capacity of P4H has not been determined on halogens other than fluorine.

In addition to P4H, other 2OG-dependent hydroxylases that catalyze defluorination were also reported, such as γ-butyrobetaine hydroxylase.[153] The defluorination process is similar to the P4H mediated reaction, which forms the keto product via fluoride elimination. The use of fluorinated substrate analogues to examine the activity of more enzymes in the 2OG-dependent superfamily seems a good strategy for further mechanistic exploration and identification of detoxification activity.

5.   C–F Bond Functionalization by Non-Heme Iron Dioxygenases

5.1.   Rieske Non-Heme Iron Dependent Dioxygenase

Rieske oxygenases belong to another class of non-heme iron-containing enzyme family that catalyze a wide variety of biotransformations in diverse organisms by utilizing molecular oxygen.[154] The most prominent reaction catalyzed by Rieske oxygenase in the literature is the *cis*-dihydroxylation of aromatic compounds, first identified in the biodegradation pathway of *Pseudomonas putida*.[155] Besides the same mononuclear iron-based catalytic center (2-His-1-carboxylate coordination) as tetrahydrobiopterin- and 2OG-dependent hydroxylases, Rieske oxygenases also bear an iron-sulfur cluster that is commonly found as a [2Fe-2S] cluster held by two cysteines and two histidines. These enzymes are typically trimeric in structure, and the iron-sulfur cluster mediates the transfer of electrons to the non-heme iron center across two different subunits, which are bridged by either a conserved aspartate or glutamate residue (**Figure 10A**).

A *cis*-dihydroxylation reaction mediated by a Rieske oxygenase enzyme involves a two-electron reduction in the presence of oxygen and NAD(P)H. A reductase extracts two electrons

from NAD(P)H to initiate the electrons transfer, and the Rieske center shuttles the electrons to the catalytic iron center potentially through the aspartate/glutamate residue.[156] Rieske dioxygenases are capable of oxidizing the four major types of aromatic compounds, including naphthalene, phenanthrene, benzoate, and toluene/biphenyl.[157] Certain Reskie oxygenases have been reported to display defluorination activity when exposed to fluorinated substrates, including toluene-1,2-dioxygenase and 2-halobenzoate-1,2-dioxygenase.[29, 35] Herein, 2-halobenzoate-1,2-dioxygenase (2HD) will be used as an example to illustrate the detailed mechanism of C–F bond cleavage promoted by Rieske dioxygenases. The 2HD enzyme controls the first step of biodegradation of 2-halobenzoate to generate a catechol by eliminating halide and CO_2 (**Figure 10B**), providing the substrate for subsequent oxidative ring cleavage by intradiol or extradiol dioxygenase enzymes.[29, 158, 159]

As shown in **Figure 11**, the proposed catalytic cycle begins with the binding of an aromatic substrate to dispel a water molecule. The resulting five-coordinated ferrous center promotes oxygen ligation to generate a ferric ion-bound superoxide intermediate, followed by reduction by the the Rieske cluster then protonation to yield a ferric hydroperoxo species. The ferric hydroperoxo species has both oxygen atoms chelated to the iron in a side-on manner, as revealed by X-ray crystallography (**Figure 10A**).[160, 161] The structural study also shows that a solvent molecule nearby may serve as the proton source.[160] Homolytic O–O bond cleavage coupled with substrate oxidation yields a ferryl-oxo species and a substrate-based radical intermediate with a hydroxyl group added to the primary substrate. The high-valent iron complex further proceeds the second oxygen coupling to the substrate radical, yielding a ferric alkoxy complex (**Figure 11**).[154, 162] It is not clear which carbon gets hydroxylated first, either the a-carbon or the fluorinated carbon, which may rely on their relative distances to the peroxide oxygen atom. Transfer of the second

electron from the Rieske cluster and protonation results in the formation of a dihydroxylated

product and regeneration of the resting state of the enzyme. Before the product is liberated from

the active site, the energetically favorable re-aromatization induces the elimination of CO_2 and

fluoride from the ring (**Figure 11**). The enzyme exhibits a very broad promiscuous substrate

selectivity. Catechol transformation has been observed in reactions of 2-fluoro-, 2-chloro-, 2-

bromo-, and 2-iodobenzoate with decreasing activity,[29] which may result from a combined effect

of steric hindrance and leaving group efficiency in the process of aromatic dehalogenation.

Another Rieske enzyme capable of C–F cleavage is toluene-1,2-dioxygenase. It has been

found that 3-fluoro-substituted benzene underwent defluorination when incubated with toluene-

2,3-dioxygenase with the formation of fluoride (**Figure 10C**).[35] Collectively, Rieske non-heme

iron oxygenase adds another member to the metalloenzymes that promote defluorination through

hydroxylation.

5.2.   Non-Heme Iron Thiol Dioxygenase

Cysteamine dioxygenase (ADO) and cysteine dioxygenase (CDO) are the only two known

mammalian thiol dioxygenases to date.[163] These enzymes exhibit many common structural and

functional features. These are non-heme iron-dependent enzymes that oxidize the thiol group of

the substrate and insert both oxygen atoms of O_2 to the same sulfur atom, leading to the production

of sulfinic acids. These thiol dioxygenases function as thiol regulators and oxygen sensors in

mammalian cells.[164-166] Structurally, the active site of ADO/CDO is centered at a mononuclear,

non-heme ferrous ion coordinated by three histidine residues along with a protein-derived,

cysteine-tyrosine (Cys-Tyr) crosslinked cofactor located in the second coordination sphere.[36, 167,

168] As shown in **Figure 12A**, the Cys-Tyr cofactor is covalently crosslinked through a thioether

bond between the side chains of a cysteine residue and a tyrosine residue (Cys93 and Tyr157 in human CDO, and Cys220 and Tyr222 in human ADO, respectively). The presence of the Cys-Tyr cofactor increases the catalytic efficiency by stabilizing substrate binding and potential intermediates.[169-172] This post-translational modification has recently been studied through the genetic code expansion method to incorporate an unnatural amino acid, 3,5-difluoro-tyrosine (F_2-Tyr), to replace the native tyrosine of the Cys-Tyr cofactor.[36, 37] This unnatural amino acid is introduced with the intention of disrupting the formation of a Cys-Tyr crosslink, since the C–F bond is more durable than the corresponding C–H bond, consequently increasing the difficulty of C–S bond formation. However, the enzyme-based oxidant is found to be sufficiently powerful, such that the added C–F bond cannot prevent the self-catalyzed formation of the Cys-Tyr cofactor. The C–F bond is cleaved in the engineered protein, resulting in a mono-fluorinated Cys-Tyr cofactor and a fluoride anion, as shown in **Figure 12B**. This finding may provide a clue as to why some fluorinated compounds are toxic and carcinogenic, even though the C–F bond is thought to be inert. Iron-containing enzymes in humans could unexpectedly dismantle the fluorine-protected molecules, resulting in toxic metabolites before reaching their intended medical targets.

The formation of the Cys-Tyr cofactor requires the presence of dioxygen and the primary substrate in both human thiol dioxygenases. An uncrosslinked ternary complex crystal structure of engineered human CDO, bound with the primary substrate and nitric oxide (**Figure 12C**), has provided mechanistic insights into the cofactor biogenesis of these thiol dioxygenases and the C–F bond cleavage mechanism. It has been proposed that a cysteinyl radical generated by the non-heme iron-bound oxidant, attacks the tyrosine aromatic ring to initiate the crosslink formation and promote C–F bond cleavage in the case of a fluorinated tyrosine.[170]

Figure 13 illustrates the mechanism of C–F bond cleavage promoted by CDO. Once the enzyme-substrate complex is formed, oxygen is activated by the iron center to produce an iron-bound superoxide. Subsequent hydrogen atom abstraction from Cys93 by ferric superoxide leads to the formation of a cysteinyl radical and an iron-bound hydroperoxide. The F_2-Tyr157 is then oxidized by the thiyl radical to form a transient difluoro-tyrosyl radical covalently bound to Cys93 through a thioether bond. In order to develop the crosslink, however, the later steps of wild-type and mono-fluorinated Cys-Tyr cofactor formation are distinct because the elimination of a proton or a fluoride differs by two electrons. In the creation of the native Cys-Tyr cofactor, the O_2 bound to the non-heme iron ion is proposed to be reduced to hydrogen peroxide.[170] While in the creation of mono-fluorinated Cys-Tyr cofactor, two electrons leave the system with the fluoride anion, and superoxide functions only as a facilitator without being consumed. After the attack by the thiyl radical, the hydroxyl group of the difluoro-tyrosyl radical is then deprotonated, forming a semiquinone-like intermediate upon fluorine elimination. One resonance form abstracts a hydrogen atom from the iron-bound hydroperoxide to generate the final, mono-fluorinated crosslinked cofactor. The iron center returns to the ferric superoxide form to proceed with oxygenation of the substrate, cysteine, forming the product, cysteine sulfinic acid (CSA). Similarly, the incorporation of 3,5-dichloro-tyrosine can also generate a mono-chlorinated cofactor with C–Cl bond cleavage; however, the efficiency of cofactor biogenesis is significantly decreased.[37]

A computational study on the cofactor biogenesis of C–F Bond cleavage in F_2-Tyr157 incorporated CDO has been recently reported.[173] The results, in general, support the mechanism proposed based on the experimental observations shown in **Figure 13**.[37, 170] The computational work agrees that the cofactor biogenesis starts from a thiyl radical on Cys93 rather than a Tyr157. The rate-limiting step is identified as the step of C-F bond dissociation with an energy barrier of

18.8 kcal/mol. An intriging derivation is proposed in the computational study, by which an F-atom transfer, from C3 to C4, in F_2-Tyr157 before the C-F bond cleavage takes place. The necessity of such an F atom migration remains unclear and requires experimental verification. The computational study also highlights the electrostatic influences of seven active site residues on the C-F bond cleavage. It is further suggested that the mutagenesis of Asp87 and Phe165 could improve defluorination efficiency by lowering the energy barrier.[173]

In addition to CDO and ADO, there are other thiol dioxygenases, such as 3-mercaptopropionic acid dioxygenase (MDO) and 2-mercaptosuccinic acid dioxygenase, which are equipped with a similar protein scaffold and iron center, *i.e.*, a mononuclear iron coordinated by three histidines.[174-177] Although the Cys-Tyr cofactor is not always present in other thiol dioxygenases, such a crosslink could be generated by a specific mutation, *e.g.,* G95C in MDO leads to the formation of an artificial Cys-Tyr cofactor.[178] It will be of interest to investigate whether MDO G95C and other thiol dioxygenases can cleave aromatic C–F bonds from exogenous ligands or their engineered Cys-Tyr cofactors.

6. Enzyme/Mediator-Based Radical Approach for Defluorination

The initiator of C–F bond cleavage in ADO/CDO is a thiyl radical generated by an iron-bound oxidant, which is distinct from the other addressed iron-dependent enzymes that directly activate fluorinated substrates with their iron centers. Such a strategy correlates to a defluorination concept with a unique radical-mediated mechanism. The most representative case of such an approach is the defluorination catalyzed by the laccase-mediated system. Laccaseis a multi-copper containing oxidase that catalyzes the one-electron oxidation of four equivalents of a substrate while reducing molecular oxygen to water.[179, 180] Laccase from *Trametes versicolor* is crystallized as a monomer,

which is organized in three sequentially arranged domains with similar β-barrel type architecture

(**Figure 14A**).[181] There is a total of four copper ions in each monomer, i.e., a mononuclear (Cu1

of Type 1), and a trinuclear (Cu2 and Cu3 of Type 3, and Cu4 of Type 2) centers. The trinuclear

copper center is deeply buried within the protein matrix and located between domains 1 and 3,

while Cu1 is embedded in domain 3 and closer to the protein surface. As sketched in **Figure 14B**,

Cu2, Cu3, and Cu4 form an isosceles triangle with Cu4 as the vertex. The anti-ferromagnetically

spin coupled Type 3 copper ions are both coordinated by three histidines and shared by a hydroxyl

ligand bridge. The Type 2 copper is coordinated by two histidines and a water ligand in a trigonal

planar configuration. Cu1 is held by a conserved His-Cys-His motif, and a methionine serves as

the fourth ligand in some cases. The reduction of dioxygen to water takes place at the trinuclear

copper site by converting a fully reduced protein-bound Cu^+ to the oxidized form (Cu^{2+}), passing

through the formation of a peroxide intermediate.[170, 171] Next, the fully oxidized enzyme slowly

catalyzes one-electron oxidation on four equivalents of the substrate at the mononuclear copper

site.[182]

In the presence of small-molecule redox mediators, the catalytic activity of laccase towards

more recalcitrant compounds is largely expanded.[183] Firstly, a mediator gets oxidized by laccase

and is stabilized in a radical form. This acts as an electron shuttle by diffusing out from the active

site to approach complex substrates. The substrates such as lignin polymer, with steric hindrance

and high redox potential, are therefore oxidized.[184] Ideally, four equivalents of mediator radicals

can be generated in each turnover. Collectively, the high output of reactive radicals enables laccase

to become a capable candidate for degrading polymers, phenolic compounds, and other

environmental contaminants. Biodegradation of per- or poly-fluorinated compounds by laccase

expressing microorganisms is of great interest while the mechanism is yet poorly understood, and

it is immature for general application.[185] However, past studies have attempted to gain the advantages of the laccase-mediator system to decompose polyfluorinated chemicals. As studied in the degradation of PFOA and perfluorooctanesulfonate (PFOS) contaminants, the synthetic mediator 1-hydroxybenzotriazole (HBT) can be used as a reducing substrate with laccase to initiate HBT radicals (**Figure 14C**), which helps to decompose polyfluorinated hydrocarbons to short chains and fluoride through radical propagation and rearrangement.[186, 187] The detailed mechanism is not discussed here since it is a non-specific radical process.

It is noteworthy that there are some fundamental challenges in the laccase-mediator system, which would need to be overcome before applications. A radical-based method will not be practically sound unless the problems of PFOA/PFOS enrichment, mediator toxicity, free radical-based oxidation reaction specificity and selectivity, and enzyme instability are all resolved. In essence, the enzyme-mediator system is genuinely an organic free radical approach. Compared with the small molecule mediator-based radical, a protein-based radical could target the substrate more specifically and effectively, as demonstrated by the example of ribonucleotide reductase.[188-191] Similar long-range, remote catalysis via protein radical chemistry has also been established in other enzyme-based catalysis.[192-196] We think that oxidizing covalently attached mediators to the enzyme may generate a well-behaved radical that could potentially be explored for radical-based defluorination.

7. Fluoroarene Scavengers Armed with Iron

The defluorination reactions catalyzed by each of the iron-containing enzymes discussed above are summarized in **Table 2**, along with the proposed reactive intermediates and their respective dehalogenation activities. It is noteworthy that most substrates have fluorine substituted on

aromatics except for 2OG-dependent hydroxylases, and a protein-bound mononuclear iron is the only metal center involved in catalysis, regardless of whether it is non-heme or heme-dependent, or in a ferrous or ferric state. As the reaction proceeds, iron oxidation to a higher valent state by oxygen or hydrogen peroxide is necessary to complete the reaction. However, the high-valent iron species is not strictly required to achieve C–F bond cleavage as long as an oxidant with a high redox potential is generated.

The fate of the fluorine atom and the identification of the final defluorinated organic products are essential for understanding the C–F bond chemistry. The cleaved fluorine atom has been exclusively detected as fluoride anion,[32, 36, 37] though the non-heme TyrH case has yet to be determined. Such consistency supports fluoride elimination directly from the aromatics and precludes the possibility of fluorine radical or cation formation during catalysis due to its instability. Therefore, although the bond dissociation energy of a C–F bond is extremely high, a heterolytic bond cleavage yielding a fluoride is anticipated in a biological system. It is also evident that most defluorination reactions mediated by these metalloenzymes are the outcome of functionalization (mainly hydroxylation) of a C–H bond, which is the original chemistry carried out by these enzymes. Aside from the single-turnover cofactor biogenesis reaction shown in ADO and CDO forming thioether bond, all of the defluorination reactions incorporate oxygen atom into the fluoroarenes, producing either a quinone/keto or hydroquinone with multiple turnovers. It is worth noting that these metalloenzymes can cleave the C–F bond *via* either an oxidative or a non-oxidative mechanism. The quinone/keto production in the cases of DHP, CYP, P4H, and potentially non-heme TyrH is considered an oxidative C–F bond cleavage; thus, it is promoted by the oxidized high-valent iron center, *i.e.*, ferryl-oxo species. On the other hand, the hydroquinone product formed by heme TyrH and 2HD is considered a non-oxidative C–F bond cleavage, which

requires additional electron supplement to balance fluoride formation, *e.g.*, oxidation of H_2O_2 and formation of CO_2. Overall, the C–F bond cleavage products presented in these metalloenzymes produce environmentally benign products, which makes them adequate to further develop into biocatalysts for fluorinated contaminants. While in drug discovery, metabolizable fluorine-containing compounds should undoubtedly sound the alarm on fluoride and resulting metabolites.

Additionally, among the metalloenzymes reviewed here, DHP is the only enzyme that performs defluorination as its natural chemistry, though fluorinated substrates are of the least reactive among halogenated substrates. The other enzymes discussed mediate oxidative C–H bond functionalization as their natural reaction, while C–F bond cleavage is either an alternate or a side reaction occurring when a fluorinated substrate is positioned in place of the native substrate. However, the fluorine substitution of the substrate significantly alters the polarity and reactivity.[2,3] Additionally, there is a two-electron difference between the departure of fluoride versus proton. Therefore, the C–F bond cleavage requires a different mechanism than the C–H bond cleavage. Although the mechanisms may share some similarities in the early stage of the steps of oxygen activation, but should diverge into different pathways afterward. It is an exciting phenomenon that predominantly, C–F bond is the most readily cleaved even though it is the most durable among all the C–X bonds in most of the enzymatic reactions except DHP. Possible explanations for this include the notion that fluorinated substrate has the highest binding affinity and the least steric effect. Also, the fluorine could act as a better leaving group at certain intermediary stages, *e.g.*, a substituted Meisenheimer complex in nucleophilic aromatic substitution (S_NAr).[197] The rate-determining step in S_NAr is typically the initial nucleophilic attack resulting in the formation of the negatively charged Meisenheimer complex. Given the high energy barrier of the Meisenheimer complex, elimination of halide is rapid once the intermediate is formed. Fluorine has the most

substantial negative inductive effect to help stabilize the negatively charged intermediate,[88] and thus facilitate the defluorination process. Such an explanation can rationale the halogen reactivity in heme TyrH (F > Cl > I) but not DHP (Br > Cl > F) because the latter forms a neutral intermediate even though both go through S_NAr. The concept that fluoride serves as a good leaving group can also be demonstrated by the example of glycosidases, the catalytic rate of which is monitored by the formation of fluoride using glycosyl fluorides as substrates.[198, 199] In addition to the cases discussed in this study, the ability of fluoride to be an excellent leaving group has also been exploited in other enzymatic systems by the design of fluorinated substrate analogues as mechanism-based inhibitors or probes.[200] CYP and non-heme TyrH are proposed to undergo electrophilic substitution while P4H, 2HD, ADO/CDO experience a radical rebound. In these mechanistic proposals, the steric effect may be the predominant determining factor for the C–F bond functionalization by the enzyme-based reactive intermediate.

It is our observation that the determinant factor whether an enzymatic system can promote C–F bond cleavage is whether it can generate the proposed reactive intermediates summarized in **Table 2** or chemically equivalent species. Hence, apart from the specific metalloenzymes aforementioned, C–F bond cleavage is anticipated in the enzymes that are capable of conducting similar oxidative chemistries. The enzyme families surveyed in this review include dioxygenase, hydroxylase, peroxidase, and peroxygenase. We expect more defluorination activity to be reported among these enzyme families because of the mutual catalytic mechanisms and reactive intermediates. The beneficial aspects of developing biocatalysts that mediate C–F bond cleavage include unveiling the defluorination activity of other known enzymes and identifying putative novel enzymes capable of C–F bond cleavage through bioinformatics studies, which could significantly expand the defluorination chemistries. The next phase to develop the knowledge for

applications may further benefit from enzyme engineering using the reported templates through direct evolution or cofactor manipulation.

8. Concluding Remarks

Although the C–F bond presents extraordinary chemical and thermal stability, several distinct classes of metal-dependent enzymes are shown to be able to cleave such a chemical bond either oxidatively or non-oxidatively. The biocatalytic defluorination reactions directly mediated by these metalloenzymes share many common features. The most apparent feature in common is their utilization of a mononuclear iron as their catalytic center. Synthetic complexes containing mono- or bi-nuclear $3d$ transition metals have been shown to catalyze C–F bond cleavage in varieties of systems,[201-206] which echos the potential defluorination reactivity of metalloenzyme with similar catalytic centers and ligand scaffold. Future discovery of other $3d$ transition metal-based or multi-mental dependent biocatalysts that mitigate the reliance on iron for C–F bond cleavage would be highly stimulating. Additionally, the majority of the discussed metalloenzymes perform defluorination reactions through hydroxylation via a highly reactive iron-oxygen complex. Oxygen activation by a metal center to generate a powerful oxidant is the common trait to activate the inert C–F bond. As for the enzyme/mediator-based radical approach, it can be a powerful defluorination method so long as the radical can be generated in a highly controlled manner. Other enzymatic or metal-complex systems capable of producing such radicals could potentially broaden such a strategy. Overall, a deeper understanding of these biocatalytic mechanisms will promote enzymatic applications as well as the development of catalysts in medicinal and environmental remediations.

Conflicts of interest

There are no conflicts to declare.

ORCID

Yifan Wang: 0000-0003-0378-2469

Aimin Liu: 0000-0002-4182-8176

References

1. R. Berger, G. Resnati, P. Metrangolo, E. Weber and J. Hulliger, *Chem. Soc. Rev.*, 2011, **40**, 3496-3508.
2. E. P. Gillis, K. J. Eastman, M. D. Hill, D. J. Donnelly and N. A. Meanwell, *J. Med. Chem.*, 2015, **58**, 8315-8359.
3. P. Shah and A. D. Westwell, *J. Enzyme Inhib. Med. Chem.*, 2007, **22**, 527-540.
4. M. Z. Hernandes, S. M. Cavalcanti, D. R. Moreira, W. F. de Azevedo Junior and A. C. Leite, *Curr. Drug Targets*, 2010, **11**, 303-314.
5. A. Analytics, *Global fluorochemical market: world market review by product type, by application, by end user industry (2019 Edition): opportunities and forecast (2019-2024)* Nov, 2019.
6. Y. Zhou, J. Wang, Z. Gu, S. Wang, W. Zhu, J. L. Acena, V. A. Soloshonok, K. Izawa and H. Liu, *Chem. Rev.*, 2016, **116**, 422-518.
7. B. Cui, S. Jia, E. Tokunaga and N. Shibata, *Nat. Commun.*, 2018, **9**, 4393.
8. J. M. Horner, *J. R. Soc. Health*, 1989, **109**, 147-150.
9. J. A. Camargo, *Chemosphere*, 2003, **50**, 251-264.
10. K. Steenland, T. Fletcher and D. A. Savitz, *Environ. Health Perspect.*, 2010, **118**, 1100-1108.
11. S. Jagtap, M. K. Yenkie, N. Labhsetwar and S. Rayalu, *Chem. Rev.*, 2012, **112**, 2454-2466.
12. P. I. Johnson, P. Sutton, D. S. Atchley, E. Koustas, J. Lam, S. Sen, K. A. Robinson, D. A. Axelrad and T. J. Woodruff, *Environ. Health Perspect.*, 2014, **122**, 1028-1039.
13. G. M. Lehmann, J. S. LaKind, M. H. Davis, E. P. Hines, S. A. Marchitti, C. Alcala and M. Lorber, *Environ. Health Perspect.*, 2018, **126**, 096001.
14. Chemical & Engineering News, Governments endorse global PFOA ban, with some exemptions, https://cen.acs.org/environment/persistent-pollutants/Governments-endorse-global-PFOA-ban/97/web/2019/05).
15. B. Kuehn, *JAMA*, 2019, **322**, 1757.
16. G. de Ruiter, K. M. Carsch, M. K. Takase and T. Agapie, *Chemistry*, 2017, **23**, 10744-10748.
17. A. Jana, P. P. Samuel, G. Tavcar, H. W. Roesky and C. Schulzke, *J. Am. Chem. Soc.*, 2010, **132**, 10164-10170.
18. S. Sahu, M. G. Quesne, C. G. Davies, M. Durr, I. Ivanovic-Burmazovic, M. A. Siegler, G. N. Jameson, S. P. de Visser and D. P. Goldberg, *J. Am. Chem. Soc.*, 2014, **136**, 13542-13545.
19. N. Suzuki, T. Fujita, K. Y. Amsharov and J. Ichikawa, *Chem. Commun.* , 2016, **52**, 12948-12951.
20. L. Zamostna, S. Sander, T. Braun, R. Laubenstein, B. Braun, R. Herrmann and P. Klaring, *Dalton Trans.*, 2015, **44**, 9450-9469.
21. I. Garcia-Bosch, R. E. Cowley, D. E. Diaz, R. L. Peterson, E. I. Solomon and K. D. Karlin, *J. Am. Chem. Soc.*, 2017, **139**, 3186-3195.
22. C. Colomban, A. Tobing, G. Mukherjee, C. Sastri, A. Sorokin and S. de Visser, *Chemistry*, 2019, **25**, 14320-14331.
23. H. Lv, Y. B. Cai and J. L. Zhang, *Angew. Chem. Int. Ed. Engl.*, 2013, **52**, 3203-3207.
24. J. Serrano-Plana, I. Garcia-Bosch, R. Miyake, M. Costas and A. Company, *Angew. Chem. Int. Ed. Engl.*, 2014, **53**, 9608-9612.

25. S. Sahu, B. Zhang, C. J. Pollock, M. Durr, C. G. Davies, A. M. Confer, I. Ivanovic-Burmazovic, M. A. Siegler, G. N. Jameson, C. Krebs and D. P. Goldberg, *J. Am. Chem. Soc.*, 2016, **138**, 12791-12802.

26. S. Huang and P. R. Jaffe, *Environ. Sci. Technol.*, 2019, **53**, 11410-11419.

27. C. D. Murphy, *Biotechnol. Lett.*, 2010, **32**, 351-359.

28. J. Liu and S. Mejia Avendano, *Environ. Int.*, 2013, **61**, 98-114.

29. S. Fetzner, R. Muller and F. Lingens, *J. Bacteriol.*, 1992, **174**, 279-290.

30. M. W. LaCount, E. Zhang, Y. P. Chen, K. Han, M. M. Whitton, D. E. Lincoln, S. A. Woodin and L. Lebioda, *J. Biol. Chem.*, 2000, **275**, 18712-18716.

31. M. Kiel and K. H. Engesser, *Appl. Microbiol. Biotechnol.*, 2015, **99**, 7433-7464.

32. Y. Wang, I. Davis, I. Shin, D. J. Wherritt, W. P. Griffith, K. Dornevil, K. L. Colabroy and A. Liu, *ACS Catal.*, 2019, **9**, 4764-4776.

33. P. J. Hillas and P. F. Fitzpatrick, *Biochemistry*, 1996, **35**, 6969-6975.

34. L. E. Bretscher, C. L. Jenkins, K. M. Taylor, M. L. DeRider and R. T. Raines, *J. Am. Chem. Soc.*, 2001, **123**, 777-778.

35. V. Renganathan, *Appl. Environ. Microbiol.*, 1989, **55**, 330-334.

36. Y. Wang, W. P. Griffith, J. Li, T. Koto, D. J. Wherritt, E. Fritz and A. Liu, *Angew. Chem. Int. Ed. Engl.*, 2018, **57**, 8149-8153.

37. J. Li, W. P. Griffith, I. Davis, I. Shin, J. Wang, F. Li, Y. Wang, D. J. Wherritt and A. Liu, *Nat. Chem. Biol.*, 2018, **14**, 853-860.

38. S. Miranda-Rojas and A. Toro-Labbe, *J. Chem. Phys.*, 2015, **142**, 194301.

39. P. Goldman, *J. Biol. Chem.*, 1965, **240**, 3434-3438.

40. P. W. Chan, A. F. Yakunin, E. A. Edwards and E. F. Pai, *J. Am. Chem. Soc.*, 2011, **133**, 7461-7468.

41. O. Tiedt, M. Mergelsberg, K. Boll, M. Muller, L. Adrian, N. Jehmlich, M. von Bergen and M. Boll, *mBio*, 2016, **7**.

42. O. Tiedt, M. Mergelsberg, W. Eisenreich and M. Boll, *Front. Microbiol.*, 2017, **8**, 2579.

43. M. Yevglevskis, G. L. Lee, J. Sun, S. Zhou, X. Sun, G. Kociok-Kohn, T. D. James, T. J. Woodman and M. D. Lloyd, *Org. Biomol. Chem.*, 2016, **14**, 612-622.

44. I. P. Solyanikova, O. V. Moiseeva, S. Boeren, M. G. Boersma, M. P. Kolomytseva, J. Vervoort, I. M. Rietjens, L. A. Golovleva and W. J. van Berkel, *Appl. Environ. Microbiol.*, 2003, **69**, 5636-5642.

45. L. Williams, T. Nguyen, Y. Li, T. N. Porter and F. M. Raushel, *Biochemistry*, 2006, **45**, 7453-7462.

46. M. F. Carvalho, M. I. Ferreira, I. S. Moreira, P. M. Castro and D. B. Janssen, *Appl. Environ. Microbiol.*, 2006, **72**, 7413-7417.

47. M. Husain, B. Entsch, D. P. Ballou, V. Massey and P. J. Chapman, *J. Biol. Chem.*, 1980, **255**, 4189-4197.

48. J. P. Driscoll, I. Aliagas, J. J. Harris, J. S. Halladay, S. Khatib-Shahidi, A. Deese, N. Segraves and S. C. Khojasteh-Bakht, *Chem. Res. Toxicol.*, 2010, **23**, 861-863.

49. S. Peelen, I. M. Rietjens, M. G. Boersma and J. Vervoort, *Eur. J. Biochem.*, 1995, **227**, 284-291.

50. Y. P. Chen, S. A. Woodin, D. E. Lincoln and C. R. Lovell, *J. Biol. Chem.*, 1996, **271**, 4609-4612.

51. D. A. Barrios, J. D'Antonio, N. L. McCombs, J. Zhao, S. Franzen, A. C. Schmidt, L. A. Sombers and R. A. Ghiladi, *J. Am. Chem. Soc.*, 2014, **136**, 7914-7925.

52. T. Malewschik, V. de Serrano, A. H. McGuire and R. A. Ghiladi, *Arch. Biochem. Biophys.*, 2019, **673**, 108079.

53. L. M. Carey, Doctor of Philosophy Doctoral thesis, North Carolina State University, North Carolina, U. S. A., 2017.

54. L. Lebioda, M. W. LaCount, E. Zhang, Y. P. Chen, K. Han, M. M. Whitton, D. E. Lincoln and S. A. Woodin, *Nature*, 1999, **401**, 445.

55. C. Wang, L. L. Lovelace, S. Sun, J. H. Dawson and L. Lebioda, *Biochemistry*, 2013, **52**, 6203-6210.

56. J. Zhao, V. de Serrano, J. Zhao, P. Le and S. Franzen, *Biochemistry*, 2013, **52**, 2427-2439.

57. A. H. McGuire, L. M. Carey, V. de Serrano, S. Dali and R. A. Ghiladi, *Biochemistry*, 2018, **57**, 4455-4468.

58. M. K. Thompson, M. F. Davis, V. de Serrano, F. P. Nicoletti, B. D. Howes, G. Smulevich and S. Franzen, *Biophys. J.*, 2010, **99**, 1586-1595.

59. E. D. Coulter, J. Cheek, A. P. Ledbetter, C. K. Chang and J. H. Dawson, *Biochem. Biophys. Res. Commun.*, 2000, **279**, 1011-1015.

60. R. Davydov, R. L. Osborne, S. H. Kim, J. H. Dawson and B. M. Hoffman, *Biochemistry*, 2008, **47**, 5147-5155.

61. J. D'Antonio and R. A. Ghiladi, *Biochemistry*, 2011, **50**, 5999-6011.

62. R. L. Osborne, G. M. Raner, L. P. Hager and J. H. Dawson, *J. Am. Chem. Soc.*, 2006, **128**, 1036-1037.

63. F. P. Guengerich, *Chem. Res. Toxicol.*, 2001, **14**, 611-650.

64. M. Foroozesh, J. Sridhar, N. Goyal and J. Liu, *Molecules*, 2019, **24**.

65. J. Belyea, L. B. Gilvey, M. F. Davis, M. Godek, T. L. Sit, S. A. Lommel and S. Franzen, *Biochemistry*, 2005, **44**, 15637-15644.

66. Z. Chen, V. de Serrano, L. Betts and S. Franzen, *Acta Crystallogr. D Biol. Crystallogr.*, 2009, **65**, 34-40.

67. M. K. Thompson, S. Franzen, R. A. Ghiladi, B. J. Reeder and D. A. Svistunenko, *J. Am. Chem. Soc.*, 2010, **132**, 17501-17510.

68. A. N. Hiner, E. L. Raven, R. N. Thorneley, F. Garcia-Canovas and J. N. Rodriguez-Lopez, *J. Inorg. Biochem.*, 2002, **91**, 27-34.

69. J. Feducia, R. Dumarieh, L. B. Gilvey, T. Smirnova, S. Franzen and R. A. Ghiladi, *Biochemistry*, 2009, **48**, 995-1005.

70. R. Dumarieh, J. D'Antonio, A. Deliz-Liang, T. Smirnova, D. A. Svistunenko and R. A. Ghiladi, *J. Biol. Chem.*, 2013, **288**, 33470-33482.

71. R. L. Osborne, M. K. Coggins, G. M. Raner, M. Walla and J. H. Dawson, *Biochemistry*, 2009, **48**, 4231-4238.

72. S. Franzen, L. B. Gilvey and J. L. Belyea, *Biochim. Biophys. Acta*, 2007, **1774**, 121-130.

73. J. D'Antonio, E. L. D'Antonio, M. K. Thompson, E. F. Bowden, S. Franzen, T. Smirnova and R. A. Ghiladi, *Biochemistry*, 2010, **49**, 6600-6616.

74. L. L. Yin, H. Yuan, C. Liu, B. He, S. Q. Gao, G. B. Wen, X. S. Tan and Y. W. Lin, *ACS Catal.*, 2018, **8**, 9619-9624.

75. K. L. Colabroy, *Biochim. Biophys. Acta*, 2016, **1864**, 724-737.

76. K. L. Connor, K. L. Colabroy and B. Gerratana, *Biochemistry*, 2011, **50**, 8926-8936.

77. J. Novotna, J. Olsovska, P. Novak, P. Mojzes, R. Chaloupkova, Z. Kamenik, J. Spizek, E. Kutejova, M. Mareckova, P. Tichy, J. Damborsky and J. Janata, *PLoS ONE*, 2013, **8**, 483-496.

78. U. Peschke, H. Schmidt, H. Z. Zhang and W. Piepersberg, *Mol. Microbiol.*, 1995, **16**, 1137-1156.

79. I. Hofer, M. Crusemann, M. Radzom, B. Geers, D. Flachshaar, X. F. Cai, A. Zeeck and J. Piel, *Chem. Biol.*, 2011, **18**, 381-391.

80. W. Li, A. Khullar, S. Chou, A. Sacramo and B. Gerratana, *Appl. Environ. Microbiol.*, 2009, **75**, 2869-2878.

81. W. Li, S. Chou, A. Khullar and B. Gerratana, *Appl. Environ. Microbiol.*, 2009, **75**, 2958-2963.

82. L. Najmanova, D. Ulanova, M. Jelinkova, Z. Kamenik, E. Kettnerova, M. Koberska, R. Gazak, B. Radojevic and J. Janata, *Folia. Microbiol. (Praha)*, 2014, **59**, 543-552.

83. F. S. Sariaslani, *Crit. Rev. in Biotechnol.*, 1989, **9**, 171-257.

84. M. Sono, M. P. Roach, E. D. Coulter and J. H. Dawson, *Chem. Rev.*, 1996, **96**, 2841-2887.

85. J. G. Leahy, P. J. Batchelor and S. M. Morcomb, *FEMS Microbiol. Rev.*, 2003, **27**, 449-479.

86. A. C. Rosenzweig and M. H. Sazinsky, *Curr. Opin. Struct. Biol.*, 2006, **16**, 729-735.

87. P. F. Fitzpatrick, *Biochemistry*, 2003, **42**, 14083-14091.

88. I. Fernandez, G. Frenking and E. Uggerud, *J. Org. Chem.*, 2010, **75**, 2971-2980.

89. D. C. Lamb, L. Lei, A. G. Warrilow, G. I. Lepesheva, J. G. Mullins, M. R. Waterman and S. L. Kelly, *J. Virol.*, 2009, **83**, 8266-8269.

90. P. Rydberg, L. Olsen and U. Ryde, *Curr. Inorg. Chem.*, 2012, **2**, 292-315(224).

91. P. Manikandan and S. Nagini, *Curr. Drug Targets*, 2018, **19**, 38-54.

92. K. Dornevil, I. Davis, A. J. Fielding, J. R. Terrell and **A. Liu**, *J. Biol. Chem.*, 2017, **292**, 13645-13657.

93. R. C. Nguyen, Y. Yang, Y. Wang, I. Davis and A. Liu, *ACS Catal.*, 2020, **10**, 1628-1639.

94. P. Urban, T. Lautier, D. Pompon and G. Truan, *Int. J. Mol. Sci.*, 2018, **19**.

95. G. M. Amaya, R. Durandis, D. S. Bourgeois, J. A. Perkins, A. A. Abouda, K. J. Wines, M. Mohamud, S. A. Starks, R. N. Daniels and K. D. Jackson, *Chem. Res. Toxicol.*, 2018, **31**, 570-584.

96. C. Xie, J. Zhou, Z. Guo, X. Diao, Z. Gao, D. Zhong, H. Jiang, L. Zhang and X. Chen, *Br. J. Pharmacol.*, 2013, **168**, 1687-1706.

97. Y. C. Huang, Y. C. Chang, C. N. Yeh and C. S. Yu, *Molecules*, 2016, **21**, 387.

98. S. M. Sephton, P. Dennler, D. S. Leutwiler, L. Mu, C. A. Wanger-Baumann, R. Schibli, S. D. Kramer and S. M. Ametamey, *Am. J. Nucl. Med. Mol. Imaging*, 2012, **2**, 14-28.

99. H. J. Ahr, L. J. King, W. Nastainczyk and V. Ullrich, *Biochem. Pharmacol.*, 1982, **31**, 383-390.

100. D. Njoku, M. J. Laster, D. H. Gong, E. I. Eger, 2nd, G. F. Reed and J. L. Martin, *Anesth. Analg.*, 1997, **84**, 173-178.

101. E. D. Kharasch and K. E. Thummel, *Anesthesiology*, 1993, **79**, 795-807.

102. A. Harkey, H. J. Kim, S. Kandagatla and G. M. Raner, *Biotechnol. Lett.*, 2012, **34**, 1725-1731.

103. T. Ohe, T. Mashino and M. Hirobe, *Drug Metab. Dispos.*, 1997, **25**, 116-122.

104. N. H. P. Cnubben, J. Vervoort, M. G. Boersma and I. M. C. M. Rietjens, *Biochem. Pharmacol.*, 1995, **49**, 1235-1248.

105. C. den Besten, P. J. van Bladeren, E. Duizer, J. Vervoort and I. M. Rietjens, *Chem. Res. Toxicol.*, 1993, **6**, 674-680.

106. I. M. Rietjens and J. Vervoort, *Chem. Biol. Interact.*, 1991, **77**, 263-281.

107.   I. M. Rietjens, B. Tyrakowska, C. Veeger and J. Vervoort, *Eur. J. Biochem.*, 1990, **194**, 945-954.
108.   K. P. Vatsis and M. J. Coon, *Arch. Biochem. Biophys.*, 2002, **397**, 119-129.
109.   A. M. Osman, S. Boeren, M. G. Boersma, C. Veeger and I. M. Rietjens, *Proc. Natl. Acad. Sci. U. S. A.*, 1997, **94**, 4295-4299.
110.   Y. Pan, *ACS Med. Chem. Lett.*, 2019, **10**, 1016-1019.
111.   S. C. Daubner, T. Le and S. Wang, *Arch. Biochem. Biophys.*, 2011, **508**, 1-12.
112.   K. E. Goodwill, C. Sabatier, C. Marks, R. Raag, P. F. Fitzpatrick and R. C. Stevens, *Nat. Struct. Biol.*, 1997, **4**, 578-585.
113.   K. E. Goodwill, C. Sabatier and R. C. Stevens, *Biochemistry*, 1998, **37**, 13437-13445.
114.   A. Liu, R. Y. N. Ho, L. Que, M. J. Ryle, B. S. Phinney and R. P. Hausinger, *J. Am. Chem. Soc.*, 2001, **123**, 5126-5127.
115.   M. J. Ryle, A. Liu, R. B. Muthukumaran, R. Y. N. Ho, K. D. Koehntop, J. McCracken, L. Que and R. P. Hausinger, *Biochemistry*, 2003, **42**, 1854-1862.
116.   M. J. Ryle, K. D. Koehntop, A. Liu, L. Que and R. P. Hausinger, *Proc. Natl. Acad. Sci. U. S. A.*, 2003, **100**, 3790-3795.
117.   M. Mantri, Z. Zhang, M. A. McDonough and C. J. Schofield, *FEBS J.*, 2012, **279**, 1563-1575.
118.   W. Yan, H. Song, F. Song, Y. Guo, C.-H. Wu, A. Sae Her, Y. Pu, S. Wang, N. Naowarojna, A. Weitz, M. P. Hendrich, C. E. Costello, L. Zhang, P. Liu and Y. Jessie Zhang, *Nature*, 2015, **527**, 539-543.
119.   P. F. Fitzpatrick, *Adv. Exp. Med. Biol.*, 1993, **338**, 81-86.
120.   P. A. Frantom, R. Pongdee, G. A. Sulikowski and P. F. Fitzpatrick, *J. Am. Chem. Soc.*, 2002, **124**, 4202-4203.
121.   M. S. Chow, B. E. Eser, S. A. Wilson, K. O. Hodgson, B. Hedman, P. F. Fitzpatrick and E. I. Solomon, *J. Am. Chem. Soc.*, 2009, **131**, 7685-7698.
122.   M. D. Krzyaniak, B. E. Eser, H. R. Ellis, P. F. Fitzpatrick and J. McCracken, *Biochemistry*, 2013, **52**, 8430-8441.
123.   K. M. Roberts and P. F. Fitzpatrick, *IUBMB Life*, 2013, **65**, 350-357.
124.   G. Guroff, J. W. Daly, D. M. Jerina, J. Renson, B. Witkop and S. Udenfriend, *Science (New York, N.Y.)*, 1967, **157**, 1524-1530.
125.   B. E. Eser, E. W. Barr, P. A. Frantom, L. Saleh, J. M. Bollinger, Jr., C. Krebs and P. F. Fitzpatrick, *J. Am. Chem. Soc.*, 2007, **129**, 11334-11335.
126.   A. J. Panay, M. Lee, C. Krebs, J. M. Bollinger and P. F. Fitzpatrick, *Biochemistry*, 2011, **50**, 1928-1933.
127.   A. Bassan, M. R. Blomberg and P. E. Siegbahn, *Chemistry*, 2003, **9**, 4055-4067.
128.   S. Kaufman, *Biochim. Biophys. Acta.*, 1961, **51**, 619-621.
129.   M. A. McDonough, C. Loenarz, R. Chowdhury, I. J. Clifton and C. J. Schofield, *Curr. Opin. Struct. Biol.*, 2010, **20**, 659-672.
130.   I. J. Clifton, M. A. McDonough, D. Ehrismann, N. J. Kershaw, N. Granatino and C. J. Schofield, *J. Inorg. Biochem.*, 2006, **100**, 644-669.
131.   J. C. Price, E. W. Barr, B. Tirupati, J. M. Bollinger, Jr. and C. Krebs, *Biochemistry*, 2003, **42**, 7497-7508.
132.   P. K. Grzyska, E. H. Appelman, R. P. Hausinger and D. A. Proshlyakov, *Proc. Natl. Acad. Sci. U.S.A.*, 2010, **107**, 3982-3987.

133.   P. J. Riggs-Gelasco, J. C. Price, R. B. Guyer, J. H. Brehm, E. W. Barr, J. M. Bollinger and C. Krebs, *J. Am. Chem. Soc.*, 2004, **126**, 8108-8109.

134.   S. D. Wong, M. Srnec, M. L. Matthews, L. V. Liu, Y. Kwak, K. Park, C. B. Bell, E. E. Alp, J. Y. Zhao, Y. Yoda, S. Kitao, M. Seto, C. Krebs, J. M. Bollinger and E. I. Solomon, *Nature*, 2013, **499**, 320-323.

135.   J. C. Price, E. W. Barr, T. E. Glass, C. Krebs and J. M. Bollinger, Jr., *J. Am. Chem. Soc.*, 2003, **125**, 13008-13009.

136.   S. Martinez and R. P. Hausinger, *J. Biol. Chem.*, 2015, **290**, 20702-20711.

137.   M. S. Islam, T. M. Leissing, R. Chowdhury, R. J. Hopkinson and C. J. Schofield, *Annu. Rev. Biochem.*, 2018, **87**, 585-620.

138.   A. A. Gottlieb, Y. Fujita, S. Udenfriend and B. Witkop, *Biochemistry*, 1965, **4**, 2507-2513.

139.   K. L. Gorres and R. T. Raines, *Anal. Biochem.*, 2009, **386**, 181-185.

140.   T. J. Smart, R. B. Hamed, T. D. W. Claridge and C. J. Schofield, *Bioorgan. Chem.*, 2020, **94**, 103386.

141.   J. S. Scotti, I. K. Leung, W. Ge, M. A. Bentley, J. Paps, H. B. Kramer, J. Lee, W. Aik, H. Choi, S. M. Paulsen, L. A. Bowman, N. D. Loik, S. Horita, C. H. Ho, N. J. Kershaw, C. M. Tang, T. D. Claridge, G. M. Preston, M. A. McDonough and C. J. Schofield, *Proc. Natl. Acad. Sci. U. S. A.*, 2014, **111**, 13331-13336.

142.   C. Y. Taabazuing, J. A. Hangasky and M. J. Knapp, *J. Inorg. Biochem.*, 2014, **133**, 63-72.

143.   W. G. Kaelin, *Annu. Rev. Biochem.*, 2005, **74**, 115-128.

144.   K. L. Gorres and R. T. Raines, *Crit. Rev. Biochem. Mol. Biol.*, 2010, **45**, 106-124.

145.   J. Myllyharju, *Ann. Med.*, 2008, **40**, 402-417.

146.   J. D. Vasta and R. T. Raines, *J. Med. Chem.*, 2018, **61**, 10403-10411.

147.   T. G. Smith and N. P. Talbot, *Antioxid Redox Signal*, 2010, **12**, 431-433.

148.   V. H. Haase, *Hemodial. Int.*, 2017, **21 Suppl 1**, S110-S124.

149.   G. H. Fong and K. Takeda, *Cell Death Differ.*, 2008, **15**, 635-641.

150.   R. Chowdhury, I. K. Leung, Y. M. Tian, M. I. Abboud, W. Ge, C. Domene, F. X. Cantrelle, I. Landrieu, A. P. Hardy, C. W. Pugh, P. J. Ratcliffe, T. D. Claridge and C. J. Schofield, *Nat. Commun.*, 2016, **7**, 12673.

151.   M. D. Shoulders and R. T. Raines, *Annu. Rev. Biochem.*, 2009, **78**, 929-958.

152.   S. K. Holmgren, K. M. Taylor, L. E. Bretscher and R. T. Raines, *Nature*, 1998, **392**, 666-667.

153.   A. M. Rydzik, I. K. Leung, G. T. Kochan, A. Thalhammer, U. Oppermann, T. D. Claridge and C. J. Schofield, *ChemBioChem*, 2012, **13**, 1559-1563.

154.   S. M. Barry and G. L. Challis, *ACS Catal.*, 2013, **3**, 2362-2370.

155.   D. T. Gibson, J. R. Koch and R. E. Kallio, *Biochemistry*, 1968, **7**, 2653-2662.

156.   R. E. Parales, J. V. Parales and D. T. Gibson, *J. Bacteriol.*, 1999, **181**, 1831-1837.

157.   L. P. Wackett, *Enzyme Microb. Tech.*, 2002, **31**, 577-587.

158.   P. Francisco, Jr., N. Ogawa, K. Suzuki and K. Miyashita, *Microbiology*, 2001, **147**, 121-133.

159.   Y. Wang, J. Li and A. Liu, *J. Biol. Inorg. Chem.*, 2017, **22**, 395-405.

160.   Y. Ashikawa, Z. Fujimoto, Y. Usami, K. Inoue, H. Noguchi, H. Yamane and H. Nojiri, *BMC Struct. Biol.*, 2012, **12**, 15.

161.   A. Karlsson, J. V. Parales, R. E. Parales, D. T. Gibson, H. Eklund and S. Ramaswamy, *Science*, 2003, **299**, 1039-1042.

162.   S. Kal and L. Que, *J. Biol. Inorg. Chem.*, 2017, **22**, 339-365.

163.   M. H. Stipanuk, C. R. Simmons, P. A. Karplus and J. E. Dominy, Jr., *Amino Acids*, 2011, **41**, 91-102.

164.   N. Masson, T. P. Keeley, B. Giuntoli, M. D. White, M. L. Puerta, P. Perata, R. J. Hopkinson, E. Flashman, F. Licausi and P. J. Ratcliffe, *Science*, 2019, **365**, 65-69.

165.   J. E. Dominy, Jr., C. R. Simmons, L. L. Hirschberger, J. Hwang, R. M. Coloso and M. H. Stipanuk, *J. Biol. Chem.*, 2007, **282**, 25189-25198.

166.   M. H. Stipanuk, I. Ueki, J. E. Dominy, Jr., C. R. Simmons and L. L. Hirschberger, *Amino Acids*, 2009, **37**, 55-63.

167.   C. R. Simmons, Q. Liu, Q. Q. Huang, Q. Hao, T. P. Begley, P. A. Karplus and M. H. Stipanuk, *J. Biol. Chem.*, 2006, **281**, 18723-18733.

168.   S. Arjune, G. Schwarz and A. A. Belaidi, *Amino Acids*, 2015, **47**, 55-63.

169.   C. M. Driggers, K. M. Kean, L. L. Hirschberger, R. B. Cooley, M. H. Stipanuk and P. A. Karplus, *J. Mol. Biol.*, 2016, **428**, 3999-4012.

170.   J. Li, T. Koto, I. Davis and A. Liu, *Biochemistry*, 2019, **58**, 2218-2227.

171.   C. G. Davies, M. Fellner, E. P. Tchesnokov, S. M. Wilbanks and G. N. Jameson, *Biochemistry*, 2014, **53**, 7961-7968.

172.   E. Siakkou, M. T. Rutledge, S. M. Wilbanks and G. N. L. Jameson, *Biochim. Biophys. Acta*, 2011, **1814**, 2003-2009.

173.   Z. Song, Y. Yue, S. Feng, H. Sun, Y. Li, F. Xu, Q. Zhang and W. Wang, *Chem. Phys. Lett.*, 2020, **750**, Article 137449.

174.   E. P. Tchesnokov, M. Fellner, E. Siakkou, T. Kleffmann, L. W. Martin, S. Aloi, I. L. Lamont, S. M. Wilbanks and G. N. Jameson, *J. Biol. Chem.*, 2015, **290**, 24424-24437.

175.   N. Bruland, J. H. Wubbeler and A. Steinbuchel, *J. Biol. Chem.*, 2009, **284**, 660-672.

176.   U. Brandt, G. Galant, C. Meinert-Berning and A. Steinbuchel, *Enzyme Microb. Technol.*, 2019, **120**, 61-68.

177.   U. Brandt, M. Schurmann and A. Steinbuchel, *J. Biol. Chem.*, 2014, **289**, 30800-30809.

178.   M. Fellner, S. Aloi, E. P. Tchesnokov, S. M. Wilbanks and G. N. Jameson, *Biochemistry*, 2016, **55**, 1362-1371.

179.   N. Santhanam, J. M. Vivanco, S. R. Decker and K. F. Reardon, *Trends Biotechnol.*, 2011, **29**, 480-489.

180.   Shraddha, R. Shekher, S. Sehgal, M. Kamthania and A. Kumar, *Enzyme Res.*, 2011, **2011**, 217861.

181.   K. Piontek, M. Antorini and T. Choinowski, *J. Biol. Chem.*, 2002, **277**, 37663-37669.

182.   E. I. Solomon, D. E. Heppner, E. M. Johnston, J. W. Ginsbach, J. Cirera, M. Qayyum, M. T. Kieber-Emmons, C. H. Kjaergaard, R. G. Hadt and L. Tian, *Chem. Rev.*, 2014, **114**, 3659-3853.

183.   A. I. Canas and S. Camarero, *Biotechnol. Adv.*, 2010, **28**, 694-705.

184.   L. P. Christopher, B. Yao and Y. Ji, *Front. Energy Res.*, 2014, **2**, 12.

185.   J. R. Parsons, M. Saez, J. Dolfing and P. de Voogt, *Rev. Environ. Contam. T.*, 2008, **196**, 53-71.

186.   Q. Luo, J. H. Lu, H. Zhang, Z. Y. Wang, M. B. Feng, S. Y. D. Chiang, D. Woodward and Q. G. Huang, *Environ. Sci. Technol. Lett.*, 2015, **2**, 198-203.

187.   Q. Luo, X. Yan, J. Lu and Q. Huang, *Environ. Sci. Technol.*, 2018, **52**, 10617-10626.

188.   J. Stubbe and W. A. van der Donk, *Chem. Biol.*, 1995, **2**, 793-801.
189.   P. Nordlund and P. Reichard, *Annu. Rev. Biochem.*, 2006, **75**, 681-706.
190.   P. A. Frey, *Annu. Rev. Biochem.*, 2001, **70**, 121-148.
191.   G. Kang, A. T. Taguchi, J. Stubbe and C. L. Drennan, *Science*, 2020, **368**, 424-427.
192.   X. Li, R. Fu, S. Y. Lee, C. Krebs, V. L. Davidson and A. Liu, *Proc. Natl. Acad. Sci. U.S.A.*, 2008, **105**, 8597-8600.
193.   E. T. Yukl, F. Liu, J. Krzystek, S. Shin, L. M. R. Jensen, V. L. Davidson, C. M. Wilmot and A. Liu, *Proc. Natl. Acad. Sci. U.S.A.*, 2013, **110**, 4569-4573.
194.   J. Geng, K. Dornevil, V. L. Davidson and A. Liu, *Proc. Natl. Acad. Sci. U.S.A.*, 2013, **110**, 9639-9644.
195.   J. Geng, I. Davis, F. Liu and A. Liu, *J. Biol. Inorg. Chem.*, 2014, **19**, 1057-1067.
196.   K. Rizzolo, S. E. Cohen, A. C. Weitz, M. M. Lopez Munoz, M. P. Hendrich, C. L. Drennan and S. J. Elliott, *Nat. Commun.*, 2019, **10**, 1101.
197.   N. A. Senger, B. Bo, Q. Cheng, J. R. Keeffe, S. Gronert and W. Wu, *J. Org. Chem.*, 2012, **77**, 9535-9540.
198.   B. Lougheed, H. D. Ly, W. W. Wakarchuk and S. G. Withers, *J. Biol. Chem.*, 1999, **274**, 37717-37722.
199.   S. J. Williams and S. G. Withers, *Carbohydr. Res.*, 2000, **327**, 27-46.
200.   R. Pongdee and H. W. Liu, *Bioorg Chem*, 2004, **32**, 393-437.
201.   E. Clot, O. Eisenstein, N. Jasim, S. A. Macgregor, J. E. Mcgrady and R. N. Perutz, *Acc. Chem. Res.*, 2011, **44**, 333-348.
202.   A. Nova, R. Mas-Balleste and A. Lledos, *Organometallics*, 2012, **31**, 1245-1256.
203.   S. Utsumi, T. Katagiri and K. Uneyama, *J. Fluor. Chem.*, 2013, **152**, 84-89.
204.   T. Ahrens, J. Kohlmann, M. Ahrens and T. Braun, *Chem. Rev.*, 2015, **115**, 931-972.
205.   Q. Shen, Y. G. Huang, C. Liu, J. C. Xiao, Q. Y. Chen and Y. Guo, *J. Fluor. Chem.*, 2015, **179**, 14-22.
206.   O. Eisenstein, J. Milani and R. N. Perutz, *Chem. Rev.*, 2017, **117**, 8710-8753.
166.   Z. Song, Y. Yue, S. Feng, H. Sun, Y. Li, F. Xu, Q. Zhang and W. Wang, *Chem. Phys. Lett.*, 2020, **750**, Article # 137449.
167.   E. P. Tchesnokov, M. Fellner, E. Siakkou, T. Kleffmann, L. W. Martin, S. Aloi, I. L. Lamont, S. M. Wilbanks and G. N. Jameson, *J. Biol. Chem.*, 2015, **290**, 24424-24437.
168.   N. Bruland, J. H. Wubbeler and A. Steinbuchel, *J. Biol. Chem.*, 2009, **284**, 660-672.
169.   U. Brandt, G. Galant, C. Meinert-Berning and A. Steinbuchel, *Enzyme Microb. Technol.*, 2019, **120**, 61-68.
170.   U. Brandt, M. Schurmann and A. Steinbuchel, *J. Biol. Chem.*, 2014, **289**, 30800-30809.
171.   M. Fellner, S. Aloi, E. P. Tchesnokov, S. M. Wilbanks and G. N. Jameson, *Biochemistry*, 2016, **55**, 1362-1371.
172.   N. Santhanam, J. M. Vivanco, S. R. Decker and K. F. Reardon, *Trends Biotechnol.*, 2011, **29**, 480-489.
173.   Shraddha, R. Shekher, S. Sehgal, M. Kamthania and A. Kumar, *Enzyme Res.*, 2011, **2011**, 217861.
174.   K. Piontek, M. Antorini and T. Choinowski, *J. Biol. Chem.*, 2002, **277**, 37663-37669.
175.   S. M. Jones and E. I. Solomon, *Cell Mol. Life Sci.*, 2015, **72**, 869-883.
176.   O. V. Morozova, G. P. Shumakovich, M. A. Gorbacheva, S. V. Shleev and A. I. Yaropolov, *Biochemistry (Mosc)*, 2007, **72**, 1136-1150.
177.   A. I. Canas and S. Camarero, *Biotechnol. Adv.*, 2010, **28**, 694-705.

178. L. P. Christopher, B. Yao and Y. Ji, *Front. Energy Res.*, 2014, **2**, 12.
179. J. R. Parsons, M. Saez, J. Dolfing and P. de Voogt, *Rev. Environ. Contam. T.*, 2008, **196**, 53-71.
180. Q. Luo, J. H. Lu, H. Zhang, Z. Y. Wang, M. B. Feng, S. Y. D. Chiang, D. Woodward and Q. G. Huang, *Environ. Sci. Technol. Lett.*, 2015, **2**, 198-203.
181. Q. Luo, X. Yan, J. Lu and Q. Huang, *Environ. Sci. Technol.*, 2018, **52**, 10617-10626.
182. J. Stubbe and W. A. van der Donk, *Chem. Biol.*, 1995, **2**, 793-801.
183. P. Nordlund and P. Reichard, *Annu. Rev. Biochem.*, 2006, **75**, 681-706.
184. P. A. Frey, *Annu. Rev. Biochem.*, 2001, **70**, 121-148.
185. N. A. Senger, B. Bo, Q. Cheng, J. R. Keeffe, S. Gronert and W. Wu, *J. Org. Chem.*, 2012, **77**, 9535-9540.
186. B. Lougheed, H. D. Ly, W. W. Wakarchuk and S. G. Withers, *J. Biol. Chem.*, 1999, **274**, 37717-37722.
187. S. J. Williams and S. G. Withers, *Carbohydr. Res.*, 2000, **327**, 27-46.
188. E. Clot, O. Eisenstein, N. Jasim, S. A. Macgregor, J. E. Mcgrady and R. N. Perutz, *Acc. Chem. Res.*, 2011, **44**, 333-348.
189. A. Nova, R. Mas-Balleste and A. Lledos, *Organometallics*, 2012, **31**, 1245-1256.
190. S. Utsumi, T. Katagiri and K. Uneyama, *J. Fluor. Chem.*, 2013, **152**, 84-89.
191. T. Ahrens, J. Kohlmann, M. Ahrens and T. Braun, *Chem. Rev.*, 2015, **115**, 931-972.
192. Q. Shen, Y. G. Huang, C. Liu, J. C. Xiao, Q. Y. Chen and Y. Guo, *J. Fluor. Chem.*, 2015, **179**, 14-22.
193. O. Eisenstein, J. Milani and R. N. Perutz, *Chem. Rev.*, 2017, **117**, 8710-8753.

Tables

Table 1. Comparison of the dehalogenation reactions catalyzed by the two histidine-ligated heme enzymes DHP and heme-dependent TyrH

	DHP	**Heme TyrH**
Cofactor	Histidine-ligated heme	Histidine-ligated heme
Reaction scheme		
Substrate	*para*-Substituted phenol	*meta*-Substituted phenol
Product	Oxidative C-X bond cleavage, quinone	Non-oxidative C-X cleavage, catechol
Source of oxygen	H_2O	H_2O_2
Dehalogenation reactivity	Br > Cl > F	F > Cl > I
Reactive species	Cpd I-like species	Ferric heme-bound hydroperoxo
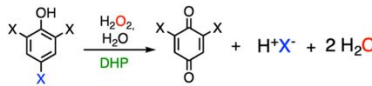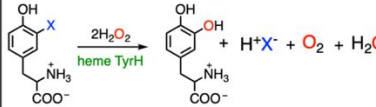
Table 2. Summary of the defluorination reactions catalyzed by iron-dependent enzymes (**A**) DHP, (**B**) heme TyrH, (**C**) CYP, (**D**) non-heme TyrH, (**E**) P4H, (**F**) 2HD (**G**) ADO/CDO. The corresponding proposed reactive intermediates are also listed as well as their dehalogenation reactivities among halogenated substrates. R = amino acid moiety. Oxygen atoms from oxidants (H$_2$O$_2$ or O$_2$) are highlighted in red.

	Reaction scheme	Proposed reactive intermediate	Dehalogenation reactivity
A	DHP (His-heme Fe^{3+}, H$_2$O$_2$, H$_2$O)	Cpd I (Fe^{IV}, His) and Cpd II (Fe^{IV}, His)	Br > Cl > F
B	heme TyrH (His-heme Fe^{3+}, H$_2$O$_2$)	Ferric hydroperoxo (Fe^{III}, His)	F > Cl > I
C	CYP (Cys-heme Fe^{2+}, NADPH, O$_2$)	Cpd I (Fe^{IV}, Cys)	F > Cl > Br
D	non-heme TyrH (Fe^{2+}, BH$_4$, O$_2$)	Non-heme ferryl-oxo (His—Fe^{IV}—Glu, His)	F > Cl > Br
E	P4H (Fe^{2+}, 2OG, O$_2$)	Non-heme ferryl-oxo (Fe^{IV}, His, Asp/Glu)	Unknown
F	2HD (Fe^{2+}, O$_2$, NAD(P)H)	Ferric hydroperoxo (His, His, Fe^{III}, Asp/Glu)	F > Cl > Br > I
G	ADO/CDO (Fe^{2+}, O$_2$)	Protein-based thiyl radical (•S—Cys)	F > Cl
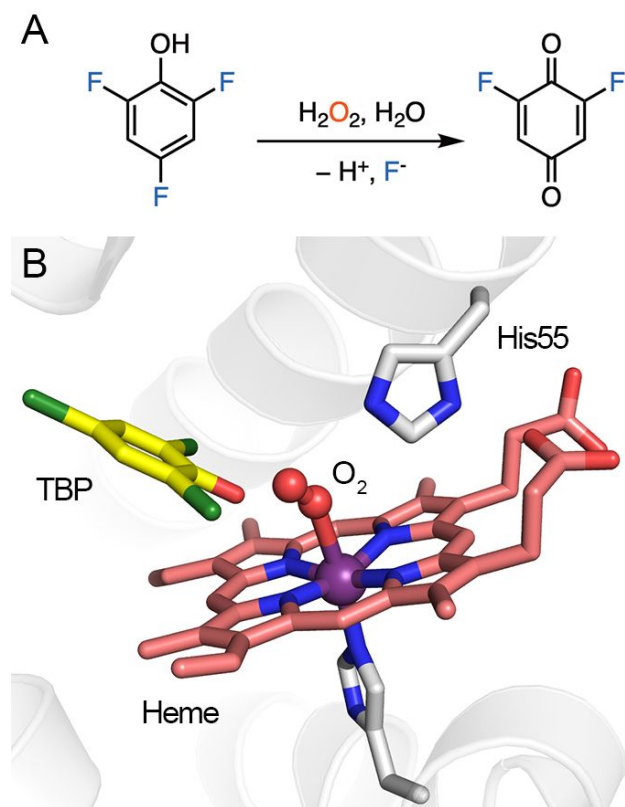
Figure 1. Dehaloperoxidase (DHP)-catalyzed reaction and its active site architecture. (**A**) Oxidative C–F bond cleavage of trifluorophenol. (**B**) A crystal structure of DHP in complex with tribromophenol (TBP) and oxygen. His55 interacts with oxygen via hydrogen bonding (PDB entry: 4FH6).

Figure 2. The C–F bond cleavage pathway promoted by DHP.
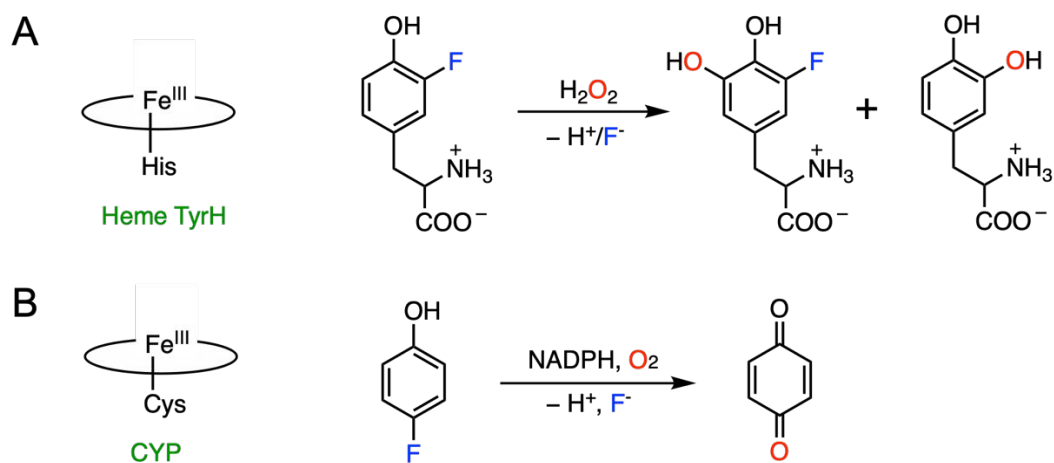
Figure 3. (**A**) Histidine-ligated heme TyrH catalyzes defluorination of 3-fluoro-tyrosine. Two products are formed with C–H and C–F bond cleavage, respectively. (**B**) Thiolate-ligated CYP catalyzes defluorination of 4-fluorophenol.
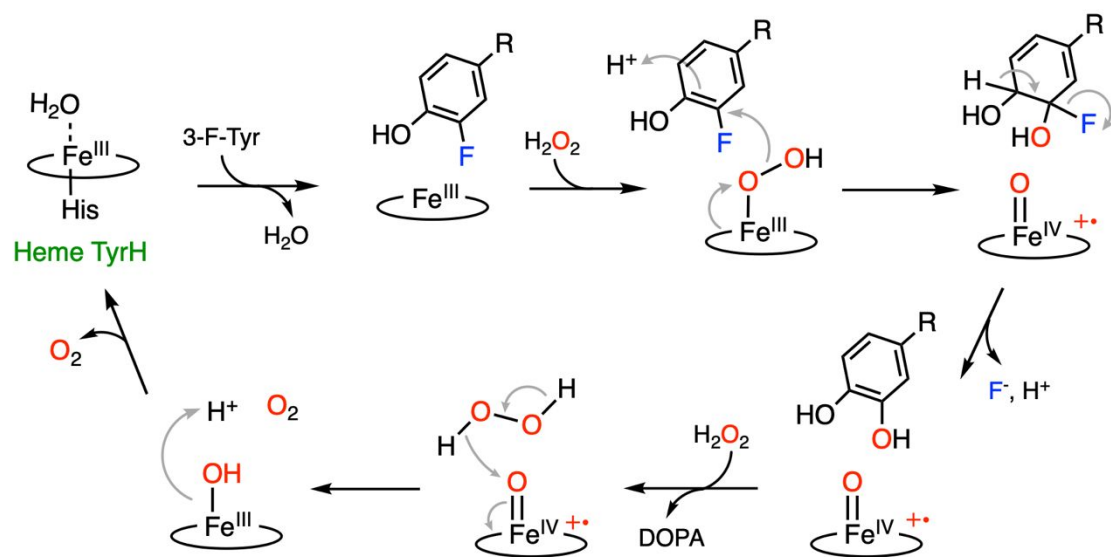
Figure 4. Proposed C–F bond cleavage mechanism promoted by heme TyrH.[32] R = amino acid moiety.
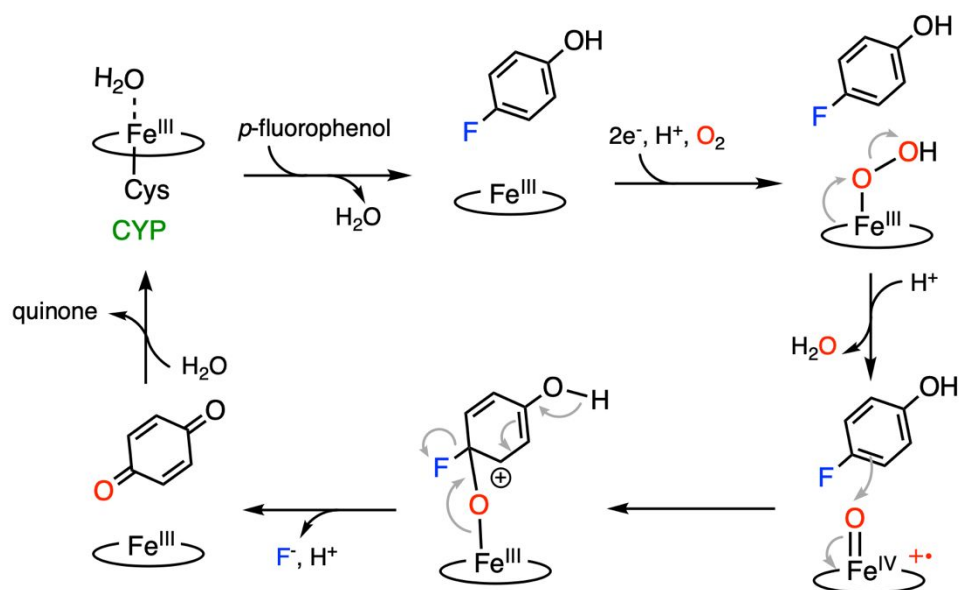
Figure 5. The mechanism of C–F bond cleavage promoted by CYP.
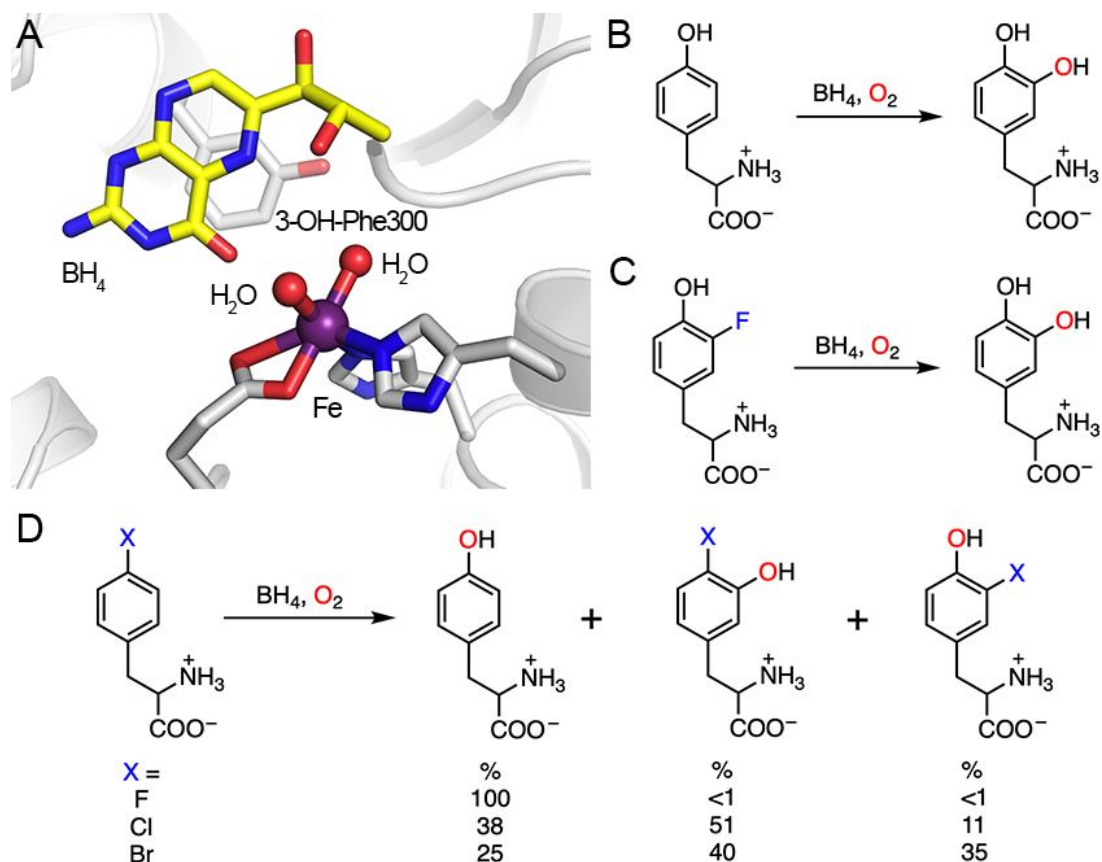
Figure 6. The active site of the non-heme TyrH and the demonstrated reactions. (**A**) Crystal structure of non-heme TyrH in complex with tetrahydrobiopterin (BH_4). Phe300 is self-hydroxylated to 3-OH-Phe300. PDB entry: 2TOH. (**B**) Natural hydroxylation of tyrosine. (**C**) Defluorination of 3-fluoro-tyrosine. (**D**) Dehalogenation of 4-halo-phenylalanine. 4-Fluoro-phenylalanine (X = F) only yields one product, tyrosine. Other halogen substitutions (X = Cl, Br) result in multiple products.
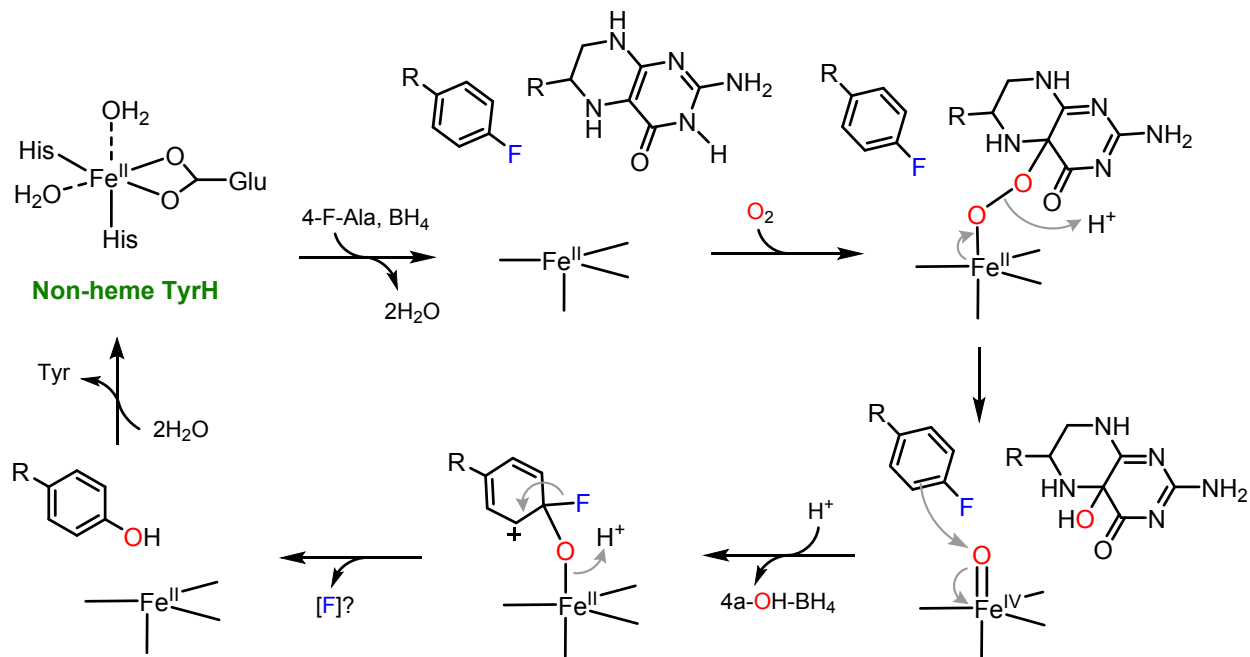
Figure 7. A plausible mechanism of C–F bond cleavage promoted by non-heme TyrH with which 4-fluoro-phenylalanine (4-F-Ala) is converted to tyrosine. BH$_4$ represents tetrahydrobiopterin. R = amino acid moiety (Note: The product derived from fluorine substitution is unclear and requires more experimental evidence for its production).
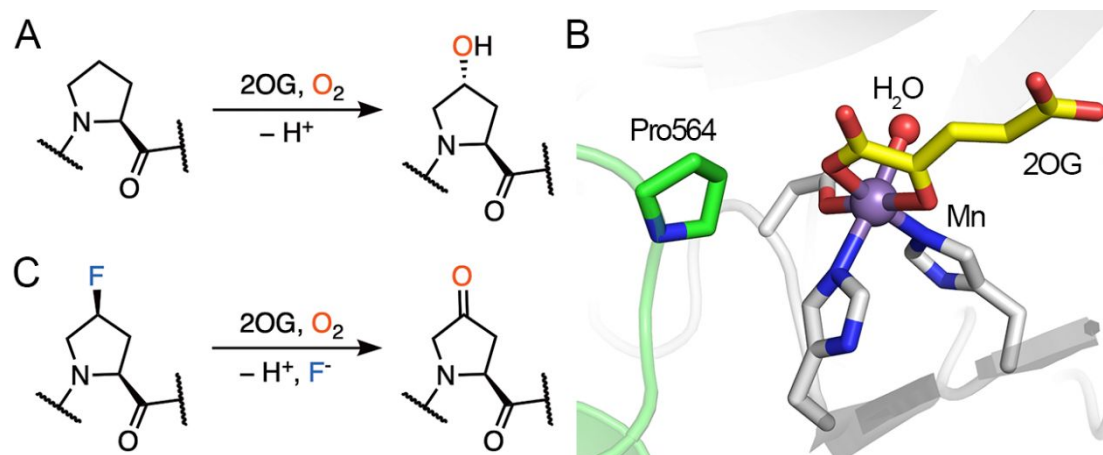
Figure 8. The demonstrated catalytic reactions and the crystal structure of P4H. (A) Native hydroxylation of P4H on a proline residue. (**B**) The catalytic active site of human P4H (white) in complex with 2OG (yellow) and a fragment of HIF peptide (green) (PDB entry: 5L9B). The catalytic iron was substituted with a manganese ion in this structure. Pro564 from HIF is the target for hydroxylation. (**C**) Defluorination of a fluorinated proline residue.
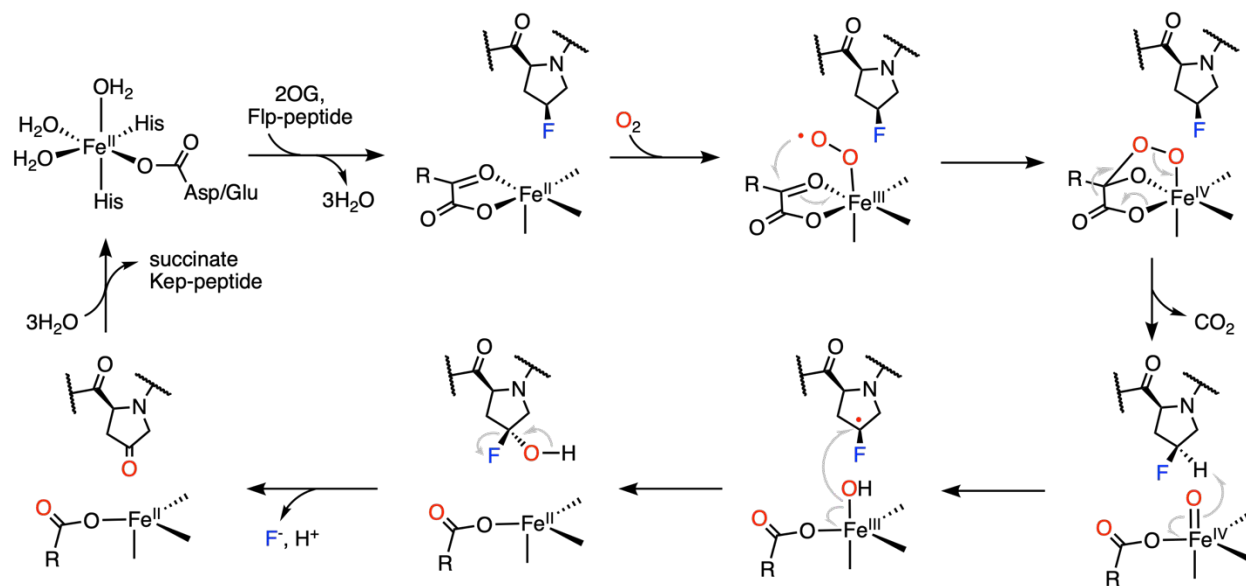
Figure 9. The mechanism of C–F bond cleavage mediated by prolyl-4-hydroxylase.
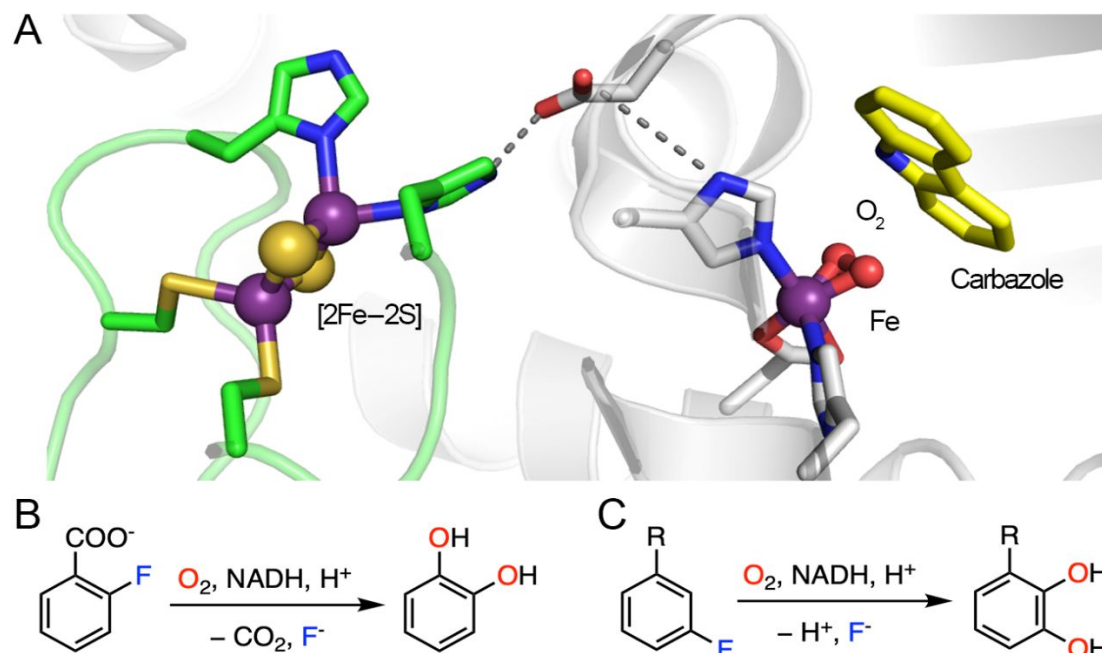
Figure 10. The architecture of Rieske oxygenase and the experimentally verified catalytic reactions. (**A**) Structure of enzyme in complex with carbazole (yellow) and oxygen. Rieske cluster and catalytic iron locate in two subunits represented by green and white ribbons, connected by an Asp residue. PDB entry: 3VMI. (**B**) Defluorination reaction catalyzed by 2HD. (**C**) Defluorination reaction catalyzed by toluene-1,2-dioxygenase. R= -CH$_3$, -CN, -X, -OCH$_3$, or -CF$_3$.
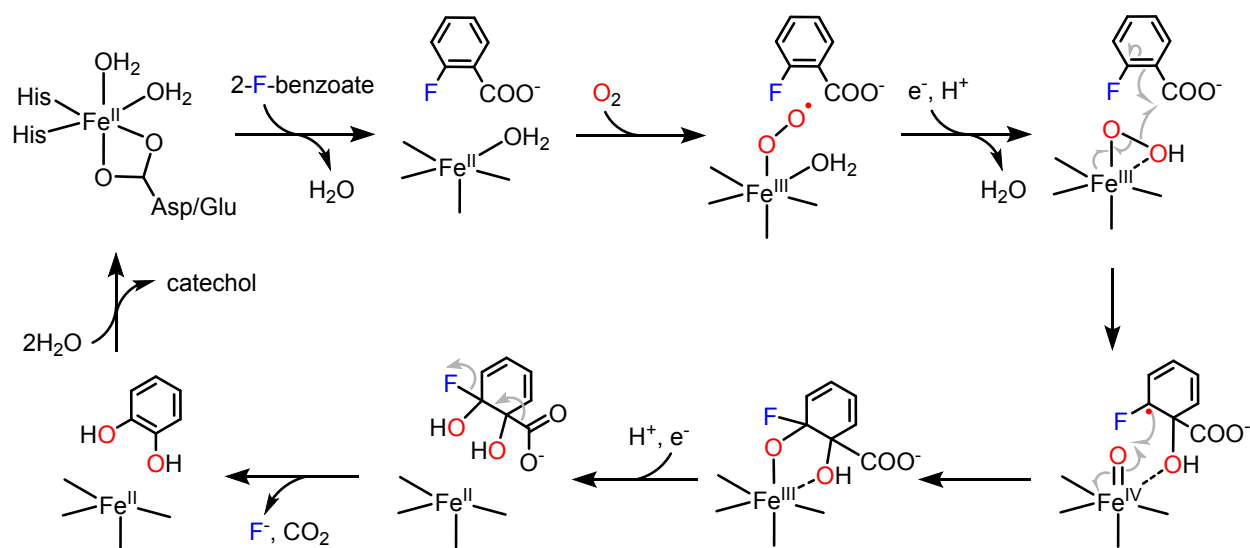
Figure 11. The mechanism of C–F bond cleavage on 2-fluoro-benzoate promoted by 2-halobenzoate-1,2-dioxygenase.
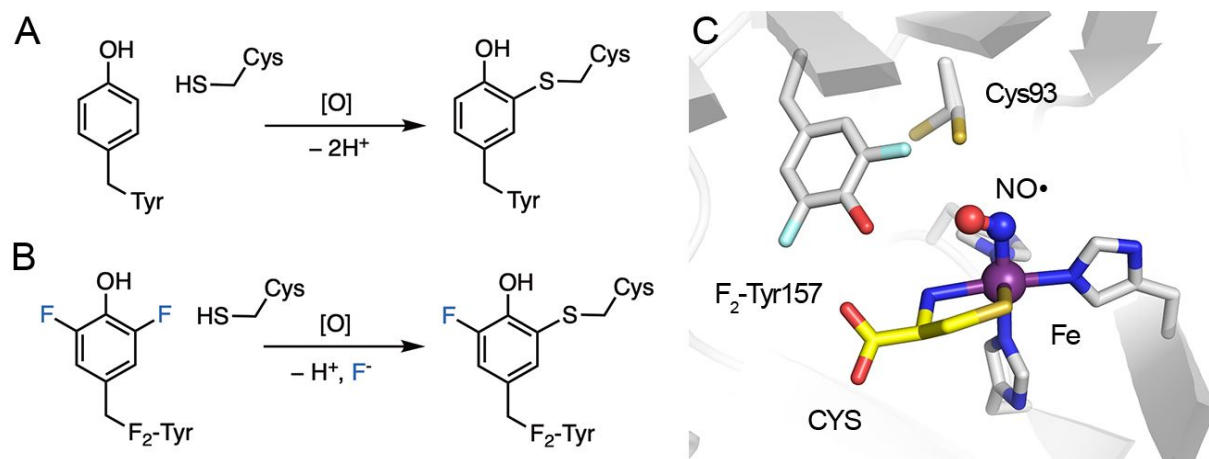
Figure 12. Cofactor biogenesis of CDO and its active site. (**A**) Crosslink formation in wild-type ADO/CDO with C–H bond cleavage. (**B**) Crosslink formation in F$_2$-Tyr ADO/CDO with C–F bond cleavage. (**C**) Crystal structure of uncrosslinked CDO bound with L-cysteine (CYS) and nitric oxide (NO•). Cys93 exhibits two conformations. PDB entry: 6BGF.
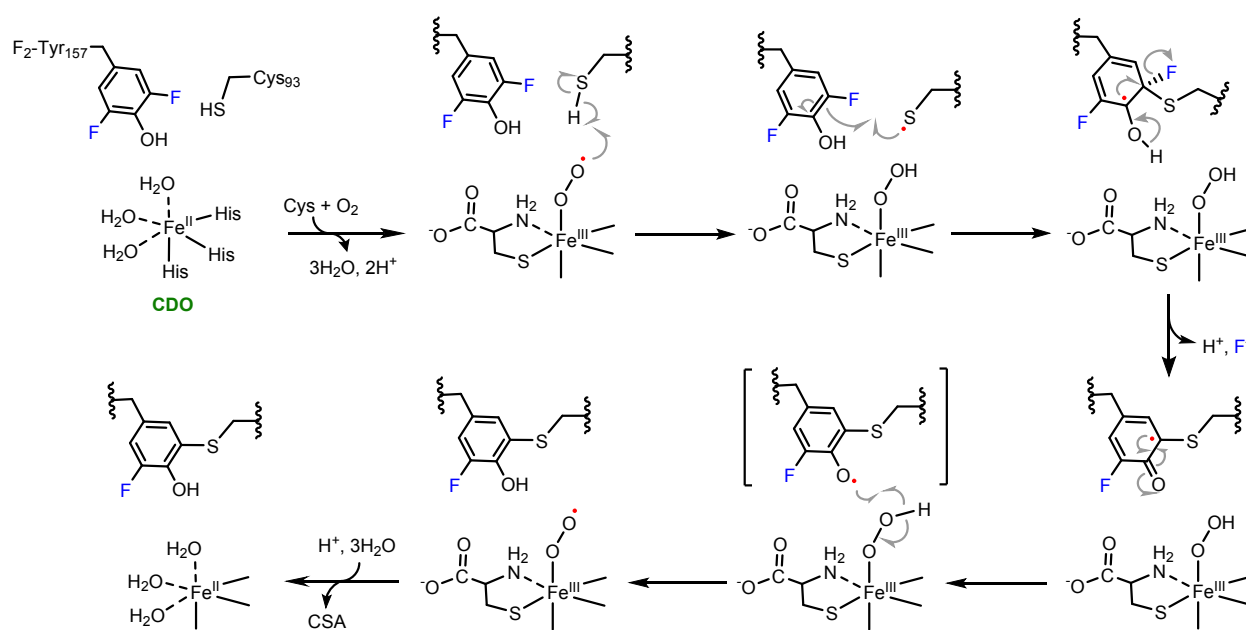
Figure 13. The mechanism of C−F bond cleavage promoted by CDO. Ferric superoxide is regenerated by after the cofactor biogenesis, and proceeds the dioxygenation of ligated substrate, forming product cysteine sulfinic acid (CSA).
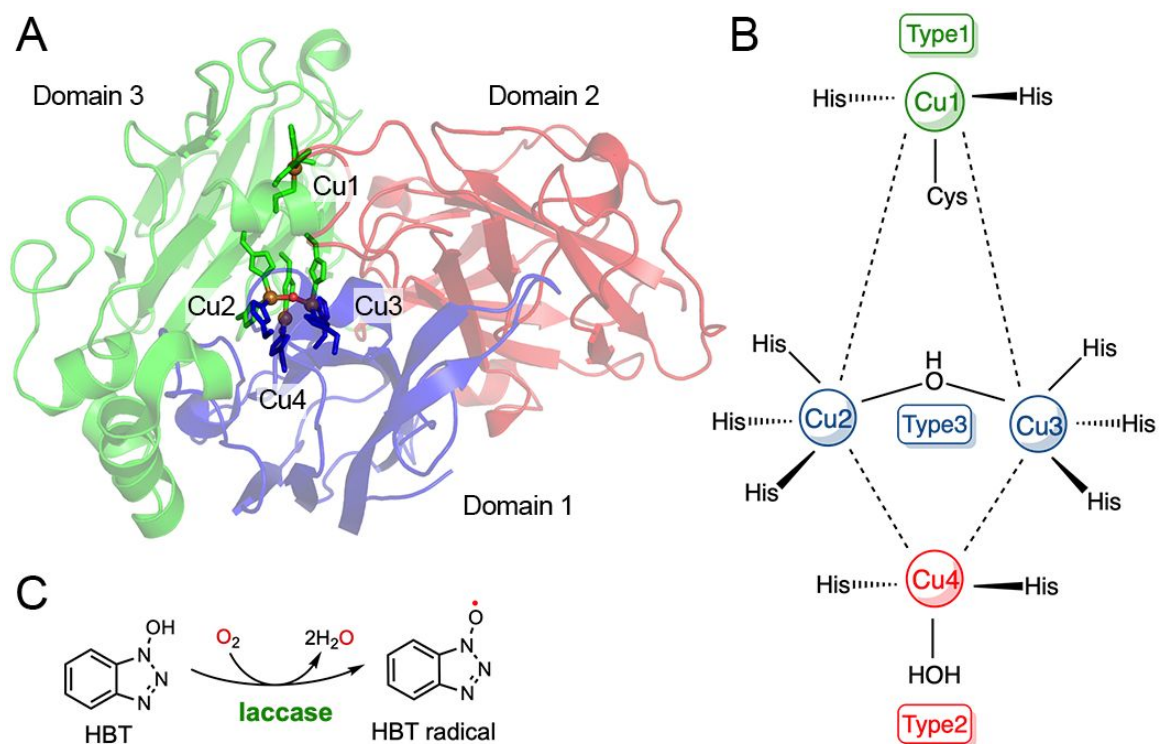
Figure 14. Laccase/HBT-based radical approach for defluorination. (**A**) A global structure of laccase from *Trametes versicolor*. It is composed of three-domain polypeptide and four copper ions. PDB entry: 1GYC. (**B**) A simplified view of the laccase active site. (**C**) Reaction scheme of HBT radical formation.
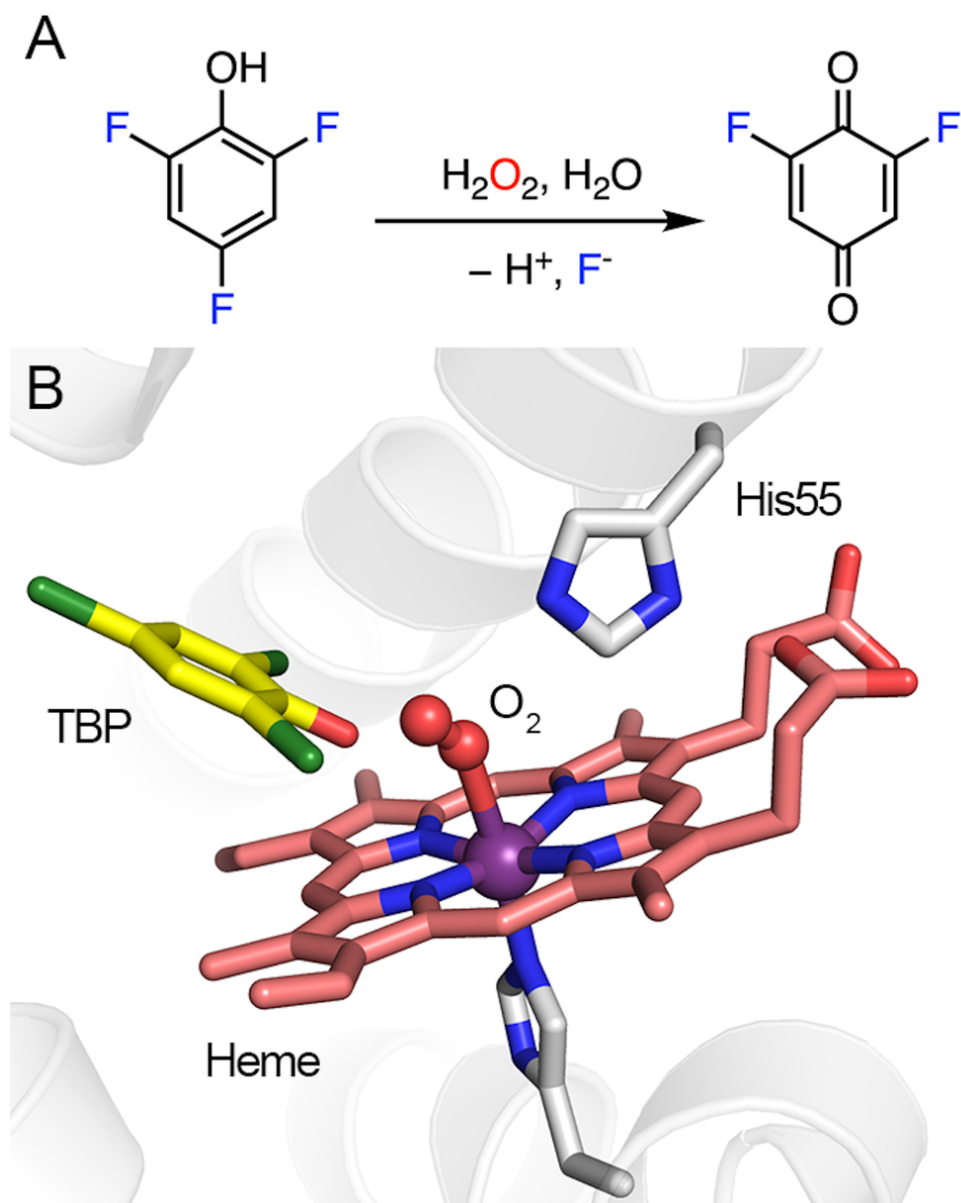
Dehaloperoxidase (DHP)-catalyzed reaction and its active site architecture. (A) Oxidative C–F bond cleavage of trifluorophenol. (B) A crystal structure of DHP in complex with tribromophenol (TBP) and oxygen. His55 interacts with oxygen via hydrogen bonding (PDB entry: 4FH6).

82x102mm (300 x 300 DPI)
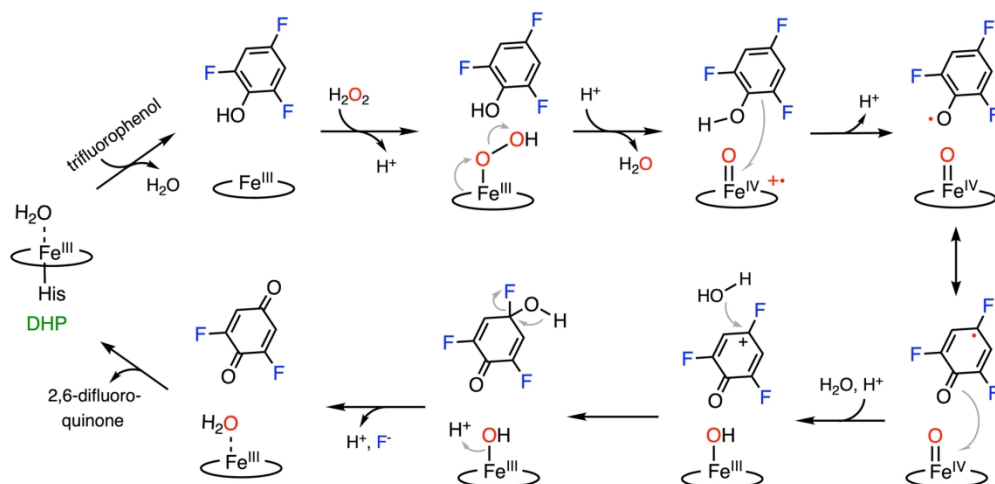
The C–F bond cleavage pathway promoted by DHP.

170x84mm (300 x 300 DPI)
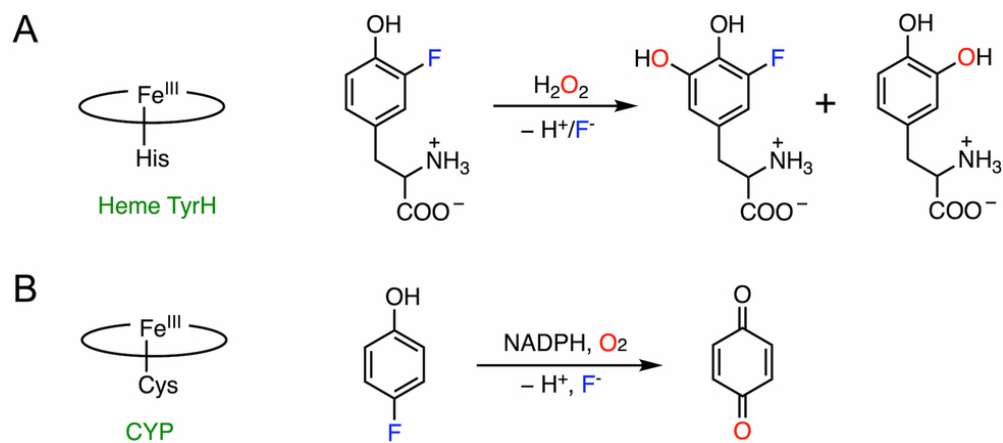
(A) Histidine-ligated heme TyrH catalyzes defluorination of 3-fluoro-tyrosine. Two products are formed with C–H and C–F bond cleavage, respectively. (B) Thiolate-ligated CYP catalyzes defluorination of 4-fluorophenol.

82x36mm (300 x 300 DPI)
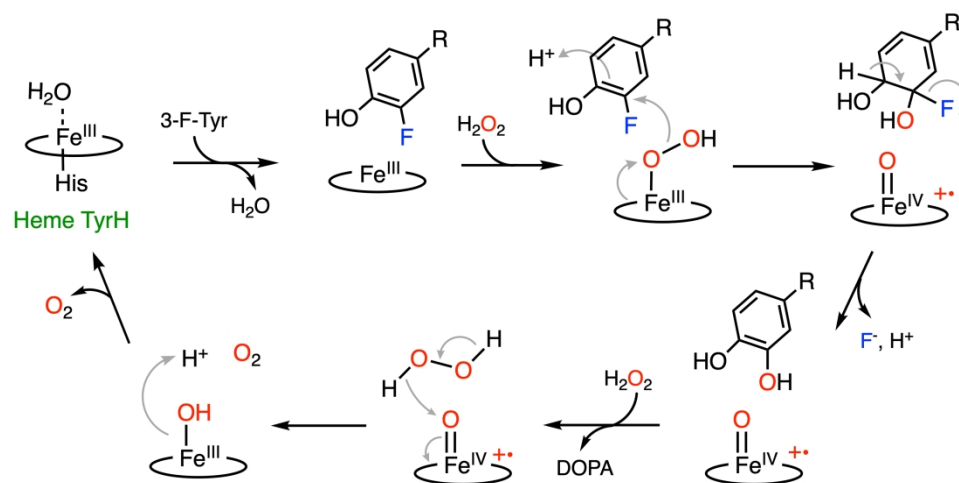
Proposed C–F bond cleavage mechanism promoted by heme TyrH (reference 32). R = amino acid moiety.

152x74mm (600 x 600 DPI)
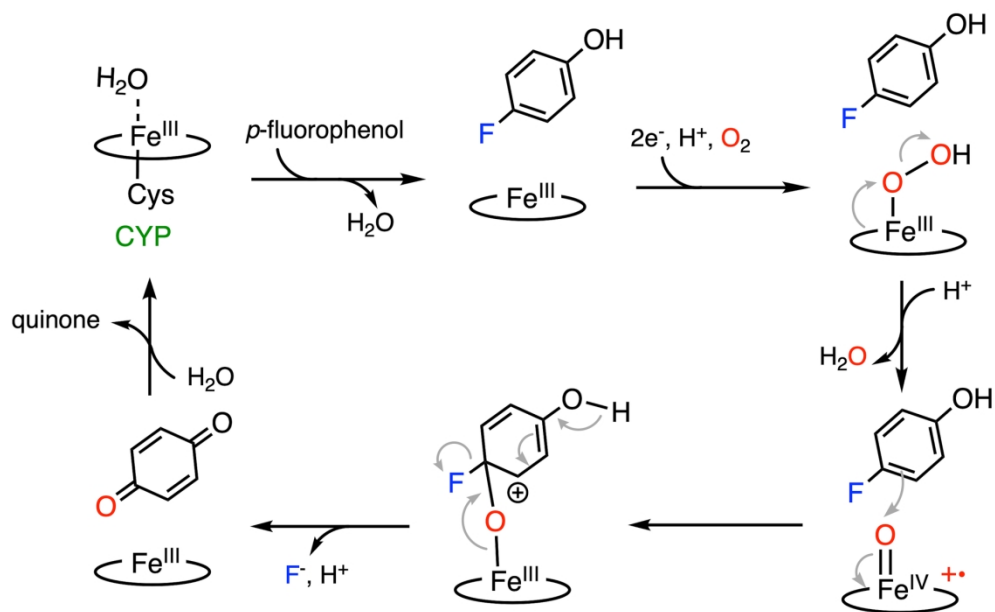
The mechanism of C−F bond cleavage promoted by CYP

170x104mm (300 x 300 DPI)
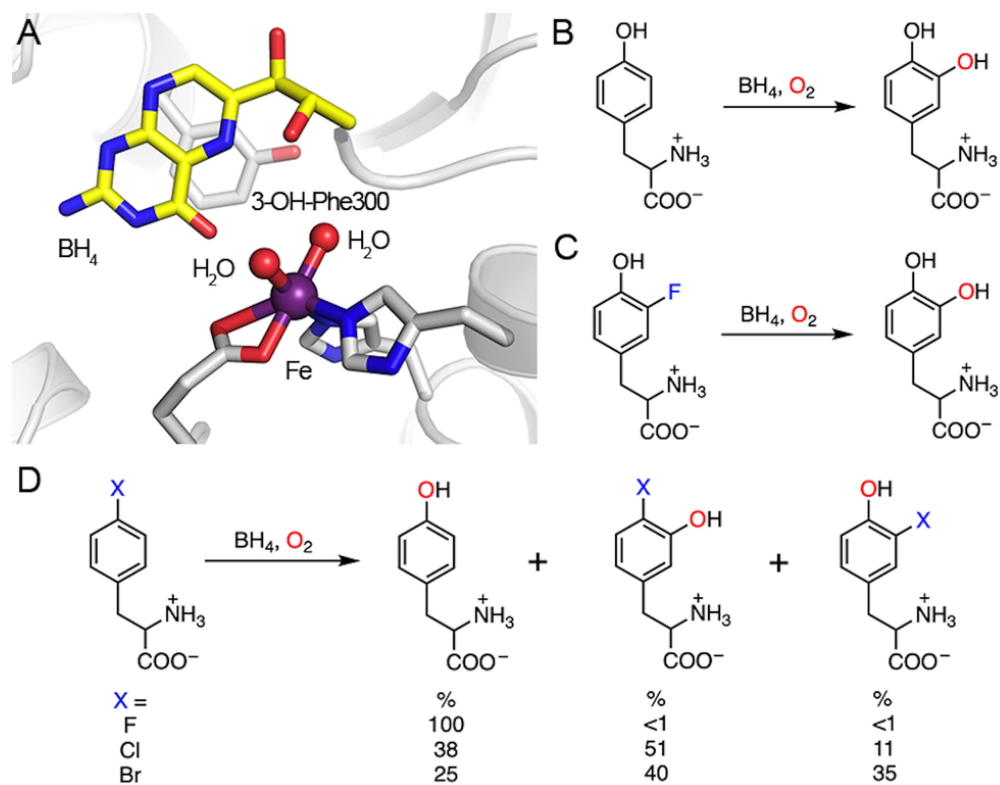
The active site of the non-heme TyrH and the demonstrated reactions. (A) Crystal structure of non-heme TyrH in complex with tetrahydrobiopterin (BH4). Phe300 is self-hydroxylated to 3-OH-Phe300. PDB entry: 2TOH. (B) Natural hydroxylation of tyrosine. (C) Defluorination of 3-fluoro-tyrosine. (D) Dehalogenation of 4-halo-phenylalanine. 4-Fluoro-phenylalanine (X = F) only yields one product, tyrosine. Other halogen substitutions (X = Cl, Br) result in multiple products.

82x64mm (300 x 300 DPI)
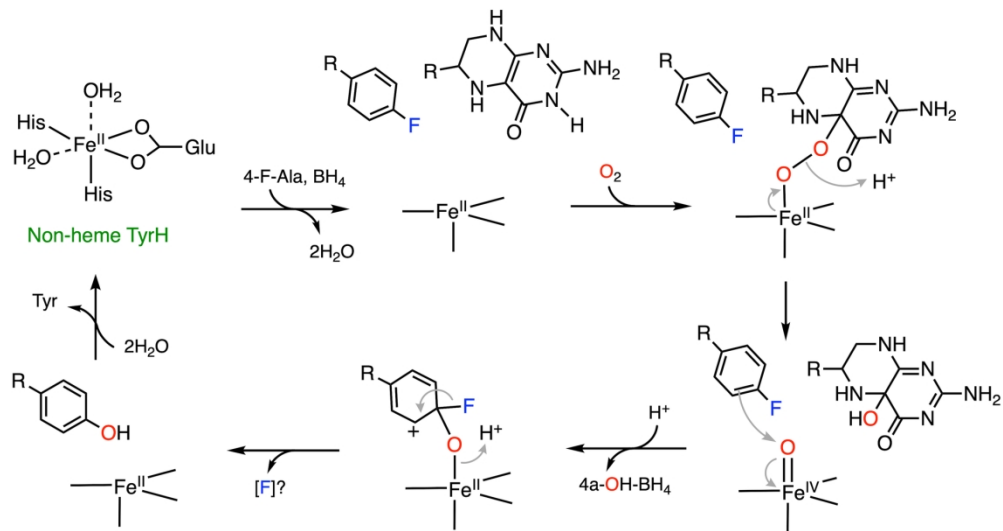
A plausible mechanism of C–F bond cleavage promoted by non-heme TyrH with which 4-fluoro-phenylalanine (4-F-Ala) is converted to tyrosine. BH4 represents tetrahydrobiopterin. R = amino acid moiety (Note: The product derived from fluorine substitution is unclear and requires more experimental evidence for its production).

170x91mm (300 x 300 DPI)
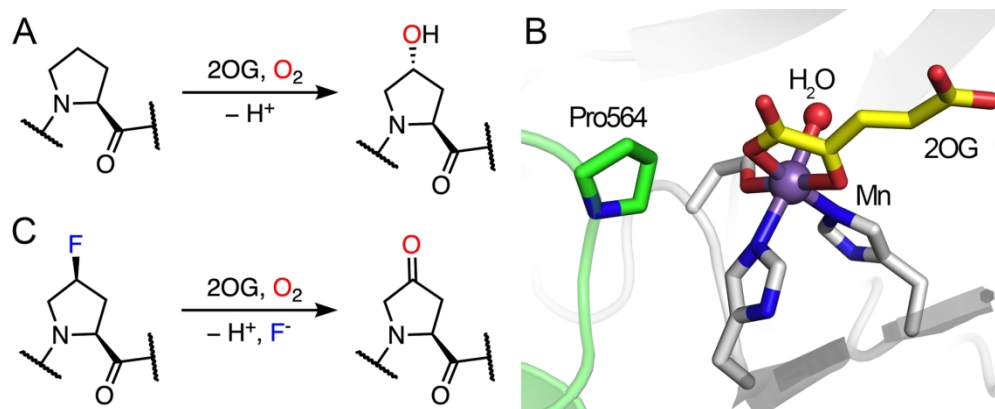
The demonstrated catalytic reactions and the crystal structure of P4H. (A) Native hydroxylation of P4H on a proline residue. (B) The catalytic active site of human P4H (white) in complex with 2OG (yellow) and a fragment of HIF peptide (green) (PDB entry: 5L9B). The catalytic iron was substituted with a manganese ion in this structure. Pro564 from HIF is the target for hydroxylation. (C) Defluorination of a fluorinated proline residue.
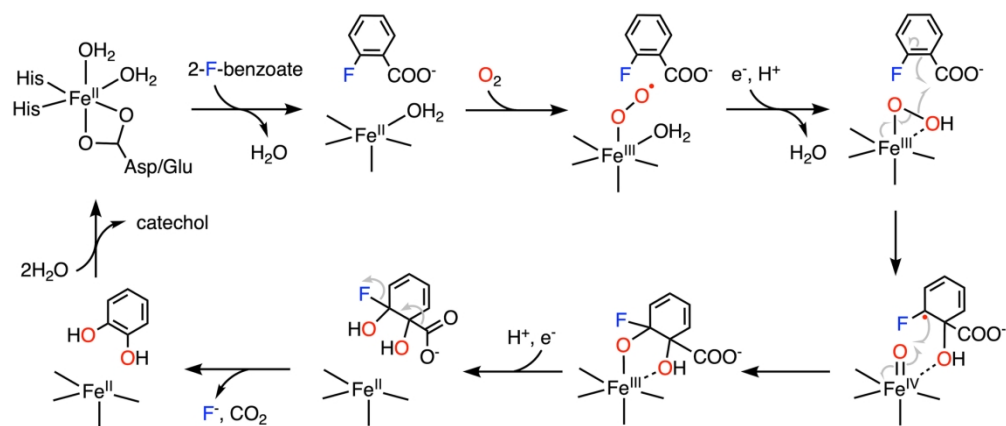
170x69mm (300 x 300 DPI)
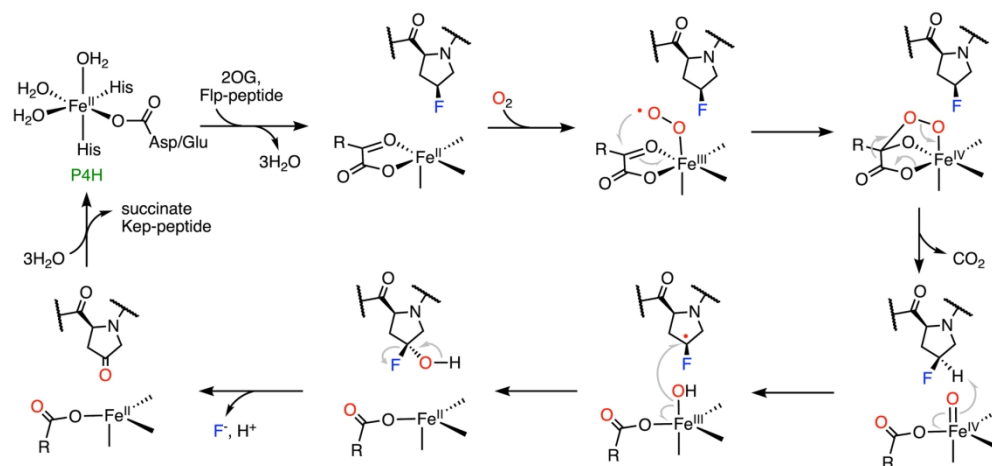
The mechanism of C–F bond cleavage mediated by prolyl-4-hydroxylase .

170x79mm (300 x 300 DPI)
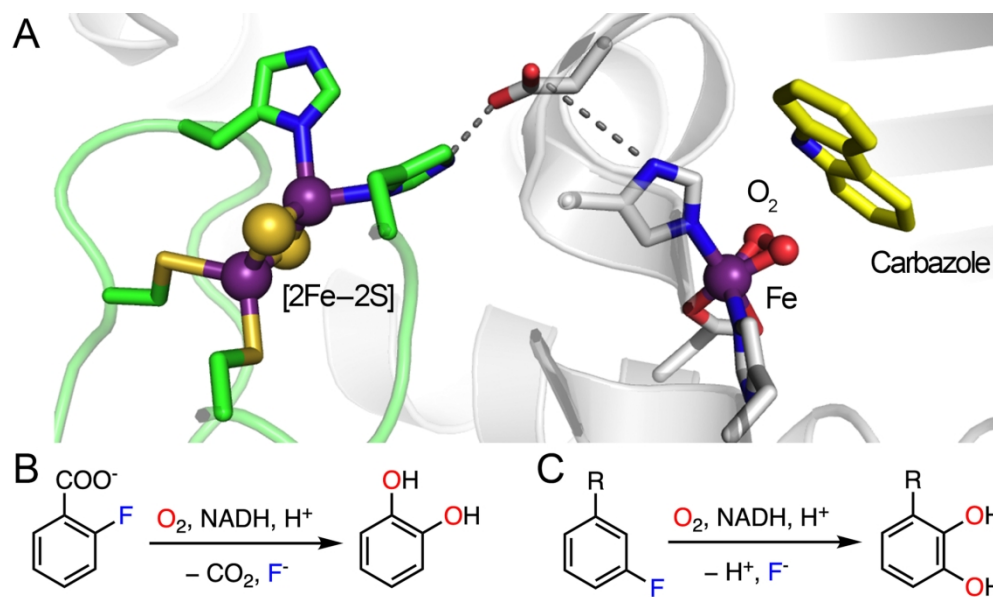
Laccase/HBT-based radical approach for defluorination. (A) A global structure of laccase from Trametes versicolor. It is composed of three-domain polypeptide and four copper ions. PDB entry: 1GYC. (B) A simplified view of the laccase active site. (C) Reaction scheme of HBT radical formation.
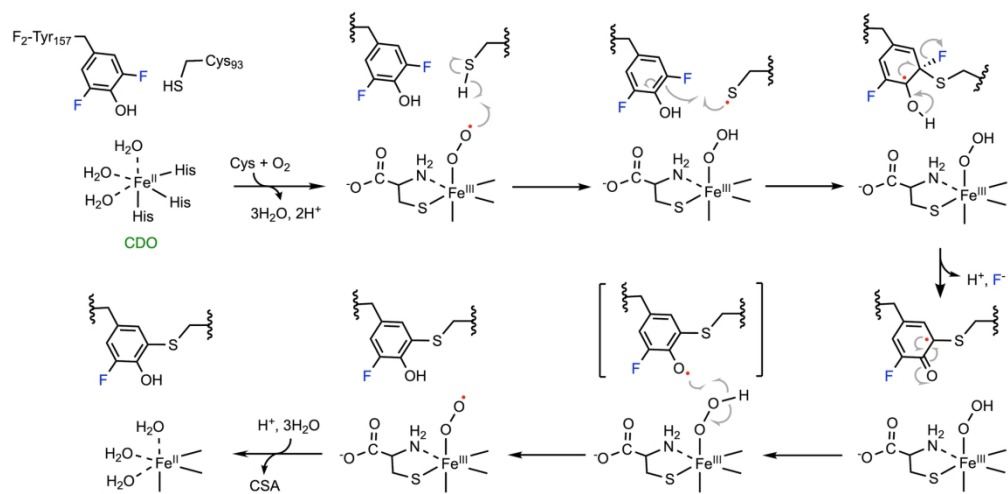
170x100mm (300 x 300 DPI)

The mechanism of C–F bond cleavage on 2-fluoro-benzoate promoted by 2-halobenzoate-1,2-dioxygenase.

170x72mm (300 x 300 DPI)
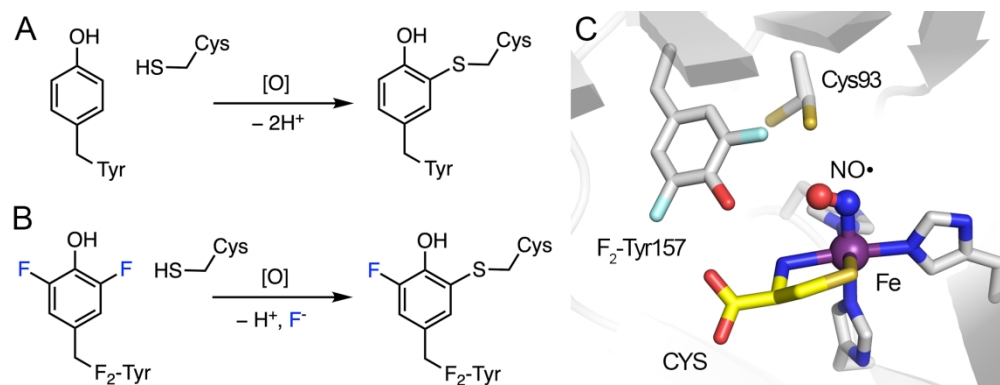
Cofactor biogenesis of CDO and its active site. (A) Crosslink formation in wild-type ADO/CDO with C−H bond cleavage. (B) Crosslink formation in F2-Tyr ADO/CDO with C−F bond cleavage. (C) Crystal structure of uncrosslinked CDO bound with L-cysteine (CYS) and nitric oxide (NO•). Cys93 exhibits two conformations. PDB entry: 6BGF.
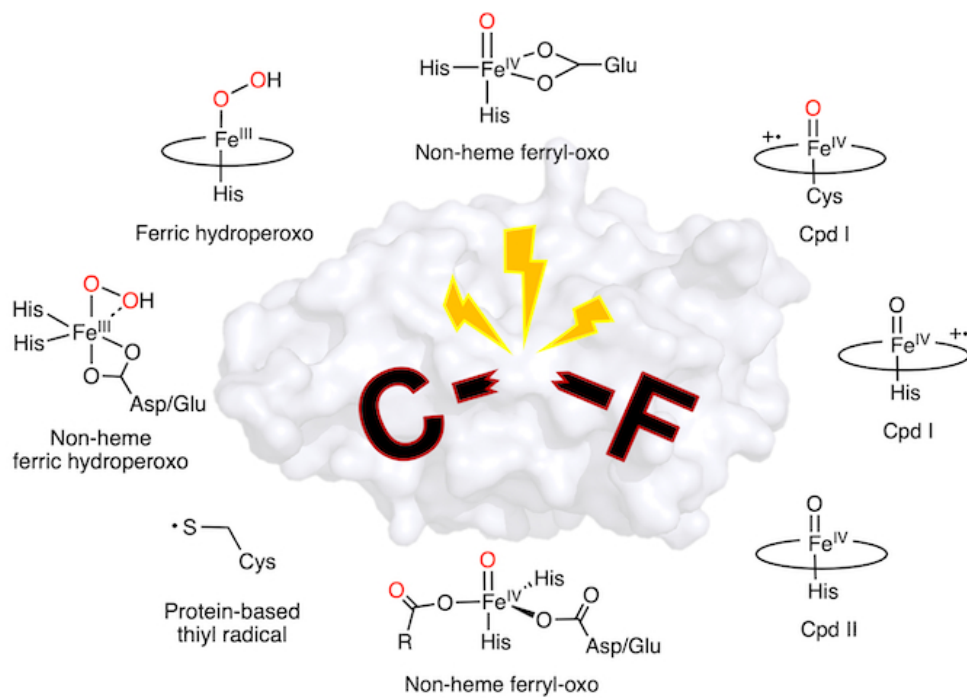
The mechanism of C–F bond cleavage promoted by CDO. Ferric superoxide is regenerated by after the cofactor biogenesis, and proceeds the dioxygenation of ligated substrate, forming product cysteine sulfinic acid (CSA).

170x84mm (300 x 300 DPI)
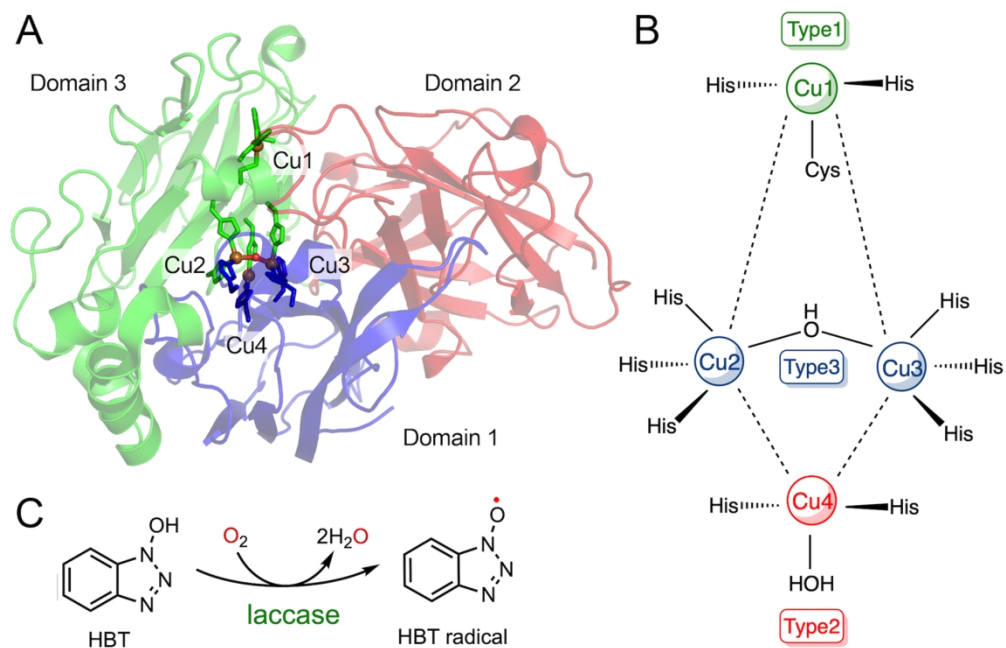
Laccase/HBT-based radical approach for defluorination. (A) A global structure of laccase from Trametes versicolor. It is composed of three-domain polypeptide and four copper ions. PDB entry: 1GYC. (B) A simplified view of the laccase active site. (C) Reaction scheme of HBT radical formation.

171x110mm (300 x 300 DPI)

58x39mm (300 x 300 DPI)